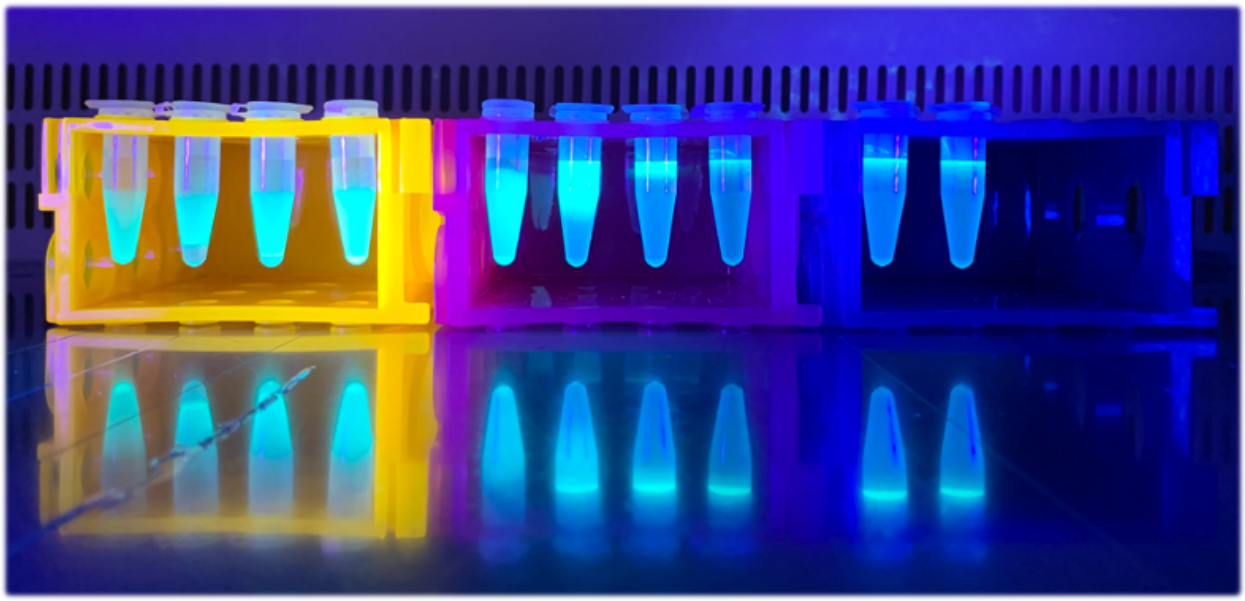

# Optimisation of bioprinting protocols for improved tissue formation

## A fight against gravity

Master's thesis in Biotechnology

CORNELIA NIELSEN-MUNK

DEPARTMENT OF LIFE SCIENCES

CHALMERS UNIVERSITY OF TECHNOLOGY
Gothenburg, Sweden 2023
www.chalmers.se

Master's thesis 2023

# Optimisation of bioprinting protocols for improved tissue formation

A fight against gravity

CORNELIA NIELSEN-MUNK


CHALMERS
UNIVERSITY OF TECHNOLOGY


Department of Life Sciences
Performed at and in cooperation with Fluicell AB
Chalmers University of Technology
Gothenburg, Sweden 2023

Optimisation of bioprinting protocols for improved tissue formation
A fight against gravity
CORNELIA NIELSEN-MUNK



Co-supervisor: Vladimir Kirejev, Fluicell R&D
Supervisor: Tatsiana Lobovkina, Fluicell R&D
Examiner: Annikka Polster, Life Sciences

Master's Thesis 2023
Department of Life Sciences
Division of Biotechnology
Chalmers University of Technology
SE-412 96 Gothenburg
Telephone +46 31 772 1000

Cover: Sedimentation of particles in solutions of different densities, with visualised fluorescence via illumination.

Typeset in LaTeX
Printed by Chalmers Reproservice
Gothenburg, Sweden 2023

Optimisation of bioprinting protocols for improved tissue formation
A fight against gravity

CORNELIA NIELSEN-MUNK
Department of Life Sciences
Chalmers University of Technology

# Abstract

Tissue generation on demand gradually transforms into reality. Generated tissues can be used for repairing native damaged tissues or be used as tissue models for evaluation of drug efficiency or toxicity. The microfluidic-based bioprinter Biopixlar, enables complex tissue generation with high-precision cell positioning. Yet, this technology could benefit from further optimisation for improved tissue formation. This project aimed to enhance printability (i.e. ease of viable cell attachment on a surface) through attempts to decrease the cell sedimentation rate, caused by gravitational force, within the printhead of Biopixlar. The project intended to exchange current printing solution (i.e. the solution in which cells are hosted during the printing process), containing polyethylene glycol (PEG) in phosphate saline buffer (PBS), to a solution with the non-ionic density gradient medium Histodenz. Mesenchymal stem cells (hMSCs) were chosen as a model cell line as they are promising cells, commonly used in regenerative medicine. Biopixlar printability was evaluated by the number of printed cells, cell viability, uniformity of printed shape and duration of printing as well as length of the printed pattern. Two printing strategies was performed, the first where continuous long lines were printed and the second where pairs of lines where printed with intermediate breaks. By the exchange of printing solution to Histodenz 12 % [w/v], the printing duration time was improved by 500-600 %. Furthermore, the shape uniformity and cell count showed increased stability between measurements when using Histodenz solutions compared to the current printing solution. In addition, cell viability after exposure to Histodenz was addressed using cell viability assays (MTS/MTT) on cultured cells supplemented with live/dead staining of printed cells. The results indicate 66-83 % cell viability, which is lower than usually obtained with currently used printing solution (over 95 %). However, these results were generated in extreme conditions (printing time) and therefore require further investigation and optimisation. In conclusion, the use of Histodenz solution 12 % [w/v] improved Biopixlar printing of hMSCs and were considered superior over PEG solution, regardless of observed reduced cell viability.

Keywords: bioprinting, printability, mesenchymal stem cells, Histodenz, polyethylene glycol, printing solution

# Acknowledgements

I want to direct my deepest thank you towards Dr Tatsiana Lobovkina, my supervisor, and Vladimir Kirejev, my co-supervisor, for all generous support along the project progression. Their expertise and supervision have given me very much appreciated guidance during the project and valuable insights for the future. I am grateful to Tatsiana for her advice in thesis writing as well as direction of the project. To Vladimir, I am impressed by your practical solutions which have had a large positive impact on the experimental part of this thesis, which I want to thank you for. Thank you for sharing your experience in the laboratory environment as well as your contribution to developing my scientific writing. Further, I want to direct a thank you towards Anton Rydberg and Adina Lupu for introducing me to work in a cell laboratory and your advice in cell cultivation. Additionally, thank you both for teaching me how to print cells using Biopixlar technology. I also thank Dr Avadhesh Kumar Singh, for the knowledge about performing an ELISA assay. Lastly, to all people working at Fluicell AB, thank you for having me. I appreciated the positive learning environment, that you all created.

Cornelia Nielsen-Munk, Gothenburg, June 2023

# Contents

# 1 Introduction

Three-dimensional (3D) printing is widely performed throughout the world and has been an expanding area since its introduction in the early 1980s [1]. The technology enables formation of geometrical structures of compatible materials [1]. Frequently printed materials, such as ceramics, metals and thermoplastics, create added value for industrial sectors such as engineering, manufacturing and medicine [2]. Due to the flexibility in the choice of material and shape, it has become a technology applicable in a wide variety of areas [1], especially with expansion in medical and biological applications [2]. It has evolved into a technology called bioprinting, which nowadays allows construction of regenerative tissues by printing cells in combination with biocompatible materials [2]. Bioprinting offers the ability to place cells in preferable arrangements with high precision [3]. By constructing tissues with a correct structure and function for its purpose, the replacement or repairing of native damaged tissues is possible [4]. In addition, disease modelling and drug toxicity testing could be based on *in vitro* tissues produced with bioprinting techniques [4]. Considering the speed of development, the field of bioprinting technology stands promising for production of tissues and organs [3].

A variety of 3D-bioprinters are now available on the market for developing tissue generation applications, allowing a range of different printing strategies [5]. Currently, the most prominent technologies among bioprinting are extrusion-, droplet-, and laser-based bioprinting [6]. However, these modalities have specific advantages and limitations that drive the need for the development of new techniques [7]. Fluicell AB focuses to contribute within the area of high precision tissue engineering with their Biopixlar®, released in 2019 [8]. The Biopixlar is a platform that allows printing of single cells and high-precision biological tissues, via a microfluidic technology based on a hydrodynamic confined flow [9]. Unlike the other technologies mentioned above, printing occurs directly in cell media or buffer, thus reducing environmental stress on the cells [10]. Prominent strengths, besides enabling printing without a bioink, is the high resolution and precision that the technology offers [9]. In the bioprinting process with the Biopixlar, multiple factors affect the outcome of tissue formation. One of the most important factors is the cell sedimentation rate within the printhead that heavily impacts the bioprinting process. Sedimentation causes effects such as uneven distribution of cells in the printhead and possible clogging. Generally, the sedimentation slows down the printing process, due to the need of recurrent pipetting of cell solution in the printhead to resuspend the cells. In order to scale up the tissue formation using the Biopixlar technology, the sedimentation problem needs to be solved or at least minimised. This thesis will fight gravity in its attempts to reduce cell sedimentation rate, via modifications of printing solution of Biopixlar technology.

## 1.1 Aim

This project aims to improve tissue patterning by optimising bioprinting protocols of the Biopixlar technology. This was deemed as high importance for the research and developmental work at Fluicell AB. The focus will be on reducing cell sedimentation

speed and consequent cell aggregation within the printhead without affecting cell attachment and retention on a substrate. With a broad perspective, the project aims to improve the quality of bioprinted tissues, as well as optimising the printing technique.

## 1.2 Goal and scope

A density gradient medium, Histodenz™ (Sigma-Aldrich®), has been evaluated to improve printing. The Histodenz has been added to polyethylene glycol in which cells are suspended in for printing, with the idea to obtain a more viscous solution. The goal has been to reach an appropriate percentage [w/v] of Histodenz that matches the single-cell density for printing. Theoretically, through matching of the solution density to the single-cell density, the sedimentation can be reduced and keep cells dispersed in the liquid for a longer period of time. However, the incorporation of Histodenz into mixtures for printing is required to not affect other crucial parameters in tissue generation. Such parameters, among others, are cell adhesion to the printing surface and cell viability. Therefore, the analysis of sedimentation, cell viability and their attachment during printing is the core of this project, in order to optimise bioprinting protocols.

The project is limited to the evaluation of human mesenchymal stem cells (hMSC), with respect to sedimentation behaviour in Histodenz. The choice of cell line was based on the fact that hMSCs often are included in developing regenerative medicine applications. Similarly, the printing and thus attachment, will solely be tested on a single type of surface, which is frequently used by the R&D department at Fluicell AB. The limitations described are due to the time plan for the project, since printing with different cell types on multiple surfaces would require additional time. Additionally, due to the time limit, printing will be performed solely in two dimensions, as it is essential to test prior to adding another dimension.

# 2 Background

Background specifically related to this project will be described in a detailed way in this section. Information about the Biopixlar technology, impacting factors in the bioprinting process and the cell line used are included topics.

## 2.1 Bioprinting technologies

Bioprinting techniques can be categorised by their printing process into extrusion-based bioprinting (EBB), droplet-based bioprinting (DBB) and laser-based bioprinting (LBB), where EBB is considered the most commonly used [11] [12]. All of these technologies use bioinks [13], a combination of cells mixed into biomaterials [14], such as hydrogels, extracellular matrix materials, additives and media [13].

Extrusion-based bioprinters, extrudes bioink through a nozzle as filaments and deposits it onto a substrate [2][11]. The extrusion-based technology allows printing of high cell densities [2], however, the shear stress experienced by the cells during dispensing has shown to decrease cell viability [4]. Furthermore, there are difficulties in achieving biological tissue models using EBB, due to limited resolution [15].

The droplet-based technology allow cell printing through a nozzle [16]. DBB deposits droplets by the use of atmospheric pressure and gravity [17]. The most common droplet-based platform is the inkjet bioprinting technology [17], which has been used for successful cell printing [18]. DBB is a simple technique offering precise deposition control and high versatility [19], however one drawback of the technology is its limitation in viscosity of bioink that can be used [20].

In laser-based bioprinting, a laser is utilised as energy source, which provides some key advantages compared to the other two techniques [21]. LBB consists of a laser generator, a mirror combined with lenses and a cell transfer module [22]. When a laser beam from the generator is focused at the cell transfer module, a bubble is generated, which allows the deposition of bioink on the substrate [22]. The technology enables printing of bioinks without using a nozzle, thereby increasing cell viability [21][22]. However, the heat of the laser can also cause damage to cells during printing [22]. Further, LBB allows material to be transferred with high precision and speed [23], yet, time-consuming if printing several cell types and the systems are associated with high costs [2].

## 2.2 Biopixlar technology

The Biopixlar is a 3D-bioprinter that allows generation of high-precision printing at single cell level [9]. With the Biopixlar, structures that mimic human tissues can be produced. Additionally, the technology can be used to develop *in vitro* applications to gain knowledge about diseases and potential drug impacts. Furthermore, Biopixlar is especially prominent in the area when using limited cell sources. In healthcare, limited cell sources could be biopsy samples [9]. Thus, Biopixlar, with its microfluidic technology, is a potential strong candidate for future clinical applications.

Biopixlar technology includes the Biopixlar printhead and a software together with a gamepad for movement control [9]. The bioprinter allow printing via the printhead, movable in three dimensions. Biopixlar has a light source and microscope with a 10x objective built in for printing visualisation [9]. In addition, there are three different modes of printing in the Biopixlar software: manual, semi-manual, and automatic modes. In manual mode, the pressures and printing speed can be regulated throughout the printing and the position of the printhead is free to adjust. For the semi-automatic mode, two parameters are predetermined before the printing process: the distance and speed. When these parameters are set the direction of printing is defined. Therefore, the printing process is done in steps of straight lines. Upon completion of the printing run (predetermined distance), it is required to provide an input to the software for the initial position for the next run (for the same pattern). In automatic mode, the printing is performed according to a predetermined pattern, where all parameters are predefined by the user, and the printing process is done when the predefined pattern has been printed.

The printhead has a central role in the Biopixlar technology. It consists of medical grade material polydimethylsiloxane (PDMS) and is a consumable, thus discarded after each completed printing session [9]. In Figure 1, a colour coded printhead is visualised. The four chambers closest to the printhead front are the delivery chambers (red, yellow, green, blue) in which different cell suspensions or other solutions can be loaded. Yet only one chamber can be activated at a time. The following four chambers (orange and pink) are intended for waste and are therefore empty at the beginning of a printing session. At the bottom of each chamber, a channel is connected leading to the printhead tip. Printing is enabled by applying positive or negative pressures on the chambers. The pressures regulate the flow within the channels of the printhead and can be adjusted for all of the chambers. The positive delivery pressure acting upon chosen delivery chamber enable printing. The positive non-delivery pressure create a slow constant flow for all delivery chambers, ensuring that chemicals do not mix at the solution junction as well as to avoid that solution flow back into any of the delivery chambers. The external vacuum is used to aspirate liquid back from the printing zone, leading to the waste recirculation chambers. The internal vacuum leads the liquid from the solution junction, within the printhead tip, to the waste switch chambers. The function of the solution junction is to enable switch between delivery chambers, without the risk of mixing solutions during printing. The magnification part of Figure 1 schematically shows the situation within the printhead tip, upon printing with chamber 1. As it can be seen from the colour coded illustration, only the solution of chamber 1 reaches the printing zone. The printing solution is delivered through the middle channel. The two side channels at the front of the printhead are used for the external vacuum which aspirates the non-attached cells into waste, to ensure a defined printing zone allowing for high precision printing. The liquid from the less pressurised delivery chambers are aspirated back via the internal vacuum, without impact on the composition of the solution aimed for printing (in activated delivery chamber).

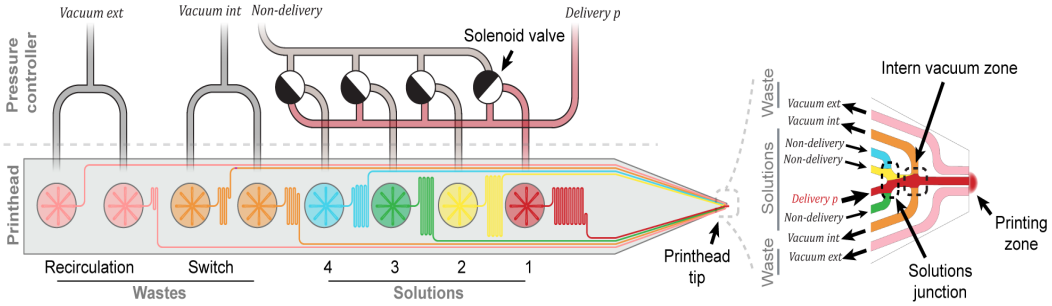


**Figure 1:** Image of the printhead, with a zoom in on the printhead tip region. The chambers are colour coded with the four delivery chambers closest to the tip (red, yellow, green and blue) followed by four waste chambers (orange and pink). Each chamber is connected to a channel where the liquid flows upon pressurisation. In the magnified part of the image, chamber one reaches the printing zone. Remaining delivery chambers are less pressurised, therefore do not reach the printing zone. The channels for internal and external vacuum leading to corresponding waste chambers are also pointed out. [Image used with permission from Fluicell].

There are other important aspects besides the printhead that are needed for printing with Biopixlar. Figure 2 (a), illustrates the printhead together with a cell dish where printing is conducted. Cell dishes are pre-coated with CAA or CAA can be introduced to the surface immediately prior the cell printing using one of the delivery chambers, see Figure 2 for the latter. CAA provides the surface with positive charges to establish attractive electrostatic forces with negative charge on the cell surfaces [24]. An already implemented coating is the mixture of poly-L-lysine and the extracellular matrix (ECM) solution of Geltrex$^{TM}$ [25]. In Figure 2 (b-c) a magnification of the front part of printhead is presented visualising the recirculating fluid zone during the cell printing procedure. Figure 2 (d-e) presents the process of multicomponent tissue printing via pressurising different delivery chambers containing separate cell lines. Note that the surface is coated before printing cells and that the dish is translating in order to print at another location. Cell printing can be performed direct in buffer, as the figure illustrates, or in cell media.

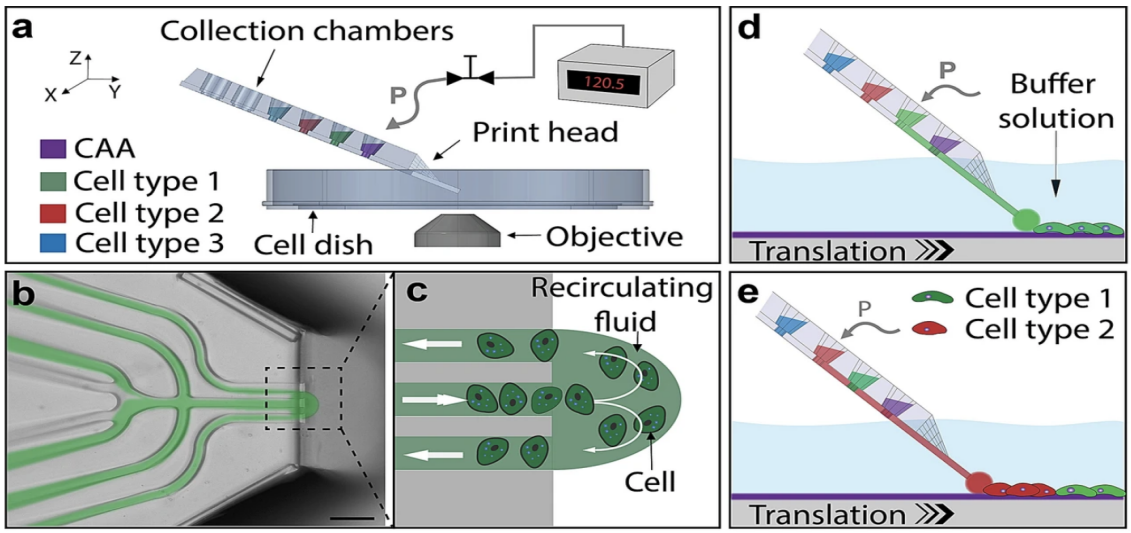


**Figure 2:** Overview of the printing equipment and printing procedure. (a) Presents the compartments that enable printing. Displayed are the objective used for visualisation and a cell dish where the pattern is printed. Printing of cell solutions occurs via applying pressure to the chambers of the printhead. The colour coding of the delivery chambers emphasises the capability of having multiple cell types in one printhead. (b-c) Illustrations show a closer perspective of the microfluidic channels in the printhead and its recirculation zone up front. In the recirculation zone, cells that do not attach to the surface are recirculated back into waste chambers. (d-e) Presents the switch between chambers to print different cell types into desired patterns within a buffer solution. Attachment of cells to the surface is possible via a cell adhesion agent (CAA). Picture obtained from [25].

## 2.3 Human mesenchymal stem cells

Stem cells possess the ability to self-renew and differentiate into mature cells of different kinds [26]. Stem cells can belong to certain categories: embryonic stem cells (ESCs), induced pluripotent stem cells (iPSCs) or adult stem cells [27]. The category of adult stem cells includes multipotent human mesenchymal stem cells (hMSCs), which can be obtained by isolation from human tissues such as bone marrow and adipose tissue, among others [27][28]. The single-cell size of MSCs varies with isolation origin, however, ranging between 15-30 $\mu$m in diameter [29]. In regenerative medicine, hMSCs are frequently used due to their potential to differentiate into mesenchymal tissues, ease of adaptation to new conditions as well as their accessibility [27][30]. Usually, hMSC differentiation results in the formation of bone (osteoblasts), cartilage (chondroblasts) and adipose tissues (adipocytes) [28]. All together, the hMSCs stands as promising candidates for developing regenerative medicine applications, whereof hMSCs were the focus of this project.

## 2.4 Printability

Printability is defined differently based on the technology it concerns and is of major importance in printing desired pattern. For instance, printability has previously been defined for extrusion-based bioprinting, as the ability to form filaments upon

extrusion [31]. However, printability, considering Biopixlar printing, could be defined as the ease of viable cell attachment and how dense cells can be deposited on a surface. Parameters to assess printability of Biopixlar is therefore number of cells printed, cell viability and duration time of printing which is connected to the length of the pattern printed. The printability of Biopixlar is today negatively affected by the fast rate of cell sedimentation within the printhead chambers. The sedimentation results in frequent need for cell resuspension, implying that cell printing appears easy right after the resuspension followed by a steady decline of printability (i.e. cells do not get printed as easily) until unfeasible to print further. Due to the fast decrease in printability over time, the determined patterns to print often come with a visible gradient in cell deposited on the surface. Unevenness of printed shape, printed cell density, cell viability and possible printing time is required to improve tissue patterning. Therefore, these parameters have together been the focus of this project in order to optimise the bioprinting protocols.

The bioprinting protocols includes usage of the compound polyethylene glycol (PEG). It is the properties of low toxicity and high biocompability that are contributory factors for the broad use of PEG in tissue engineering [32]. Using PEG solution for Biopixlar printing often results in cell viability over 95 % [9]. However, to improve the printability, this project evaluates the exchange of PEG to Histodenz. According to the producer protocol of Histodenz (Sigma Aldrich), it has been tested to possess very low toxicity and is described to be suitable in combination with cells.

# 3 Materials and Methods

This section will provide the information on materials and methodology used for the experimental parts of this project and the related preparations. Initially, preparatory procedures will be described, followed by the three main experimental parts: viability and survivability assays of hMSCs, a sedimentation experiment, and printability tests. The first two experimental parts aimed to support the last crucial step in improving tissue patterning. Lastly, the concluding image analysis follows.

## 3.1 Preparatory procedures

Described preparatory procedures in this section are relevant for specific experimental parts. The procedure described in section 3.1.1 was performed prior to the experiments that required cells. Section 3.1.2, describes the stock solutions used. Lastly, section 3.1.3 describe the procedure performed prior to printability tests.

### 3.1.1 Media composition and cell culturing

Mesenchymal stem cells (hMSCs)(PromoCell cat: C-12972) were used for optimisation of printing protocols. Cells were grown according to the producer protocol, where passages between 3-7 were used for the experiments. The complete medium for hMSC was mesenchymal stem cell growth medium 2 (PromoCell cat: C-28009), supplemented with antibiotics-antimycotics (1X)(Gibco cat: 15240062). Cultivation of hMSCs was carried out in T25 and T75 flasks and incubated in 5 % $CO_2$ at 37 °C. hMSCs detachment was performed with accutase (Fisher cat: A1110501). Cell culture and detachment were performed according to the standard operating procedure (SOP) of Fluicell AB. Detached cells were counted with a Burker chamber and dilutions were made accordingly to reach desired cell concentrations.

### 3.1.2 Stock solutions of Histodenz and polyethylene glycol (PEG)

Histodenz™ (Sigma-Aldrich® cat: D2158) was used in phosphate buffer saline (PBS)(1X)(Cytiva cat: SH30256.02) to obtain a stock solution of 0.8 mol/L. The stock solution was further diluted to working concentrations that varied based on the experiment. The Histodenz stock solution was stored in a refrigerator, however adjusted to room temperature prior to each experimental use. Additionally, the Histodenz solution was lightly vortexed prior to use. For a stock solution of polyethylene glycol (PEG) (Alfa Aesar cat: A17541.30) a 2X concentration (30 mg/ml) was prepared in PBS and stored at room temperature.

### 3.1.3 Preparations for bioprinting

Prior to each printing session, purging was required for every new printhead utilised according to the printing protocol of Fluicell AB. Purging of printheads, with milli-Q water in all chambers, was conducted in an automatic purging unit (180 mbar for 1.50 minute). The applied pressure of the purging unit forced the loaded liquid into the printhead channels. Thus, air was removed from the printhead channels

enabling printing. After the purging step, the milli-Q water was removed from the waste chambers while exchanged with the test solution of the experiment for the delivery chambers. However, only one of the delivery chambers contained hMSCs. The test solution was either PEG or Histodenz, however, the Histodenz concentrations differed among experimental runs. Cell suspension, Histodenz and PEG solution were prepared separately in double concentration (2X). Printing solutions were obtained by mixing equal volumes of cell suspension (2X) (800 000 hMSCs / 50 $\mu$l, SOP Fluicell) with Histodenz solution (2X) or PEG (2X), respectively. The printhead wells that did not contain any cells were filled with respective Histodenz or PEG solution of appropriate concentrations diluted in PBS.

Petri dishes with plastic surface (ibidi cat: 80,156) were used for printing. The 35 mm dishes with grid pattern (500x500 $\mu$m) had been pre-coated with 0.5 mg/ml poly-L-lysine (PLL, Sigma-Aldrich P6282) and 75 $\mu$g/ml Geltrex (Gibco cat: A15696-01) prior to use for improved adherence.

## 3.2 Viability and survivability assays

MTS [3-(4,5-dimethylthiazol-2-yl)-5-(3-carboxymethoxyphenyl)-2-(4-sulfophenyl)-2H-tetrazolium] assays in 96-well plates were conducted to address potential toxicity related to Histodenz. The MTS methodology was verified by a round of MTT [3-(4,5-dimethylthiazol-2-yl)-2,5-diphenyltetrazolium bromide] assay and a duplicate plate. As assay kits were provided from Abcam®(cat: ab197010, cat: ab211091) with related protocols, the assays were conducted accordingly. However, the chemical exposure times were adjusted to match the maximum length, 3 hours, of Biopixlar printing procedures at Fluicell AB. For signal detection, a SpectraMax® iD3 Multi-Mode Microplate Reader was used. Thus, four plate arrangements were analysed for hMSCs. Plate 1 and 2, were analysed with MTS and MTT, respectively, to determine the viability (readout 2 h after Histodenz exposure) of hMSCs. Survivability (readout 24 h after Histodenz exposure) of hMSCs in Histodenz solution was addressed in plate 3, while plate 4 verified that the signal was proportional to the number of seeded cells in an MTS viability set-up. Furthermore, the number of replicates, which were 4 or 6 wells per solution, was determined by the availability of hMSCs on the day of the experiment. The plates also included controls, where a gradient of DMSO and the dependence on the media were addressed. Details of the plate arrangements can be found in Appendix A.

The preparation of the mixtures for each plate was carried out from a stock DMSO (100 % [v/v]), a stock solution of Histodenz (0.8 mol/L) and PBS (1X), all diluted in hMSC medium, respectively. PBS samples were included in plate 3 to consider the different volumes of media in the Histodenz mixtures. The tested Histodenz concentration range was based on the similarity between the theoretical Histodenz densities in the product protocol and the single cell densities found in the literature. Single-cell densities have previously been measured to be in a range of 1.03-1.12 g/cm$^3$ [33], where cells with a smaller radius were in the upper range of the interval. Therefore, due to the relatively large radius of hMSCs, the Histodenz solutions of 8 % (density: 1.04 g/cm$^3$) and 18 % (density: 1.09 g/cm$^3$) was used as initial

concentrations. Higher Histodenz concentrations, such as 30 % and 40 %, were included to enable the detection of potential higher toxicity effects of Histodenz.

## 3.3 Sedimentation of fluorescent particles

Thermo Scientific$^{TM}$ Fluoro-Max Dyed Green Aqueous Fluorescent Particles (Fisher cat: G1000) were used to observe gravitational (1 x g) sedimentation in Histodenz solution. The particles served to mimic the nature of cell sedimentation, despite differences in properties. The diameter of the particles was 10 $\mu$m, while the particle density was 1.05 g/cm$^3$. The particles were left to sediment in Histodenz concentrations [w/v] of 4 %, 8 %, 10 %, 14 %, 18 %, 22 %, 26 % and 30 %. The controls were PBS and PEG 1.5 % [w/v]. All of these test solutions were prepared in separate (1.5 ml, conical) tubes. The concentration interval was chosen to be large to capture the turning point where the particles no longer sediment. The PEG sample mimics the standard printing solution of Fluicell AB, while the PBS sample aims to visualise the phenomenon when no added compound is present to reduce sedimentation. Equal volumes of particle suspensions were added to each tube and left to sediment for three hours at room temperature. The three-hour time point was based on the maximum printing time at Fluicell AB. Limited printing time avoids a major reduction in cell health, which could arise from printing when the cells are kept outside an incubator and in the absence of media. Subsequently, the visualisation of the sedimentation of fluorescent particles was enabled by UV illumination.

## 3.4 Printability of hMSCs in Histodenz solution

Experimental assessment of the printability was made using two different printing strategies in the Biopixlar® software. The strategies were (1) printing continuous lines in semi-automatic mode and (2) printing lines in automatic mode with intermediate breaks. For both strategies, printing occurred at dishes containing 2 ml PBS. Printed solutions for each experimental run was determined based on previous experiments. The initial concentrations of Histodenz were chosen based on the experimental result of the fluorescent particles. In the experiments that followed, the concentrations of Histodenz were slightly adjusted towards an appropriate concentration for hMSC printing. Such concentration was defined to be when cell sedimentation occurred at a lower rate compared to PEG. Testing printing solutions of different viscosity, such as different concentrations of Histodenz compared to PEG, can affect the recirculating fluid flow (i.e. the size of the recirculating fluid zone shown in Figure 1 of Appendix B). Further, viscosity differences between solutions loaded in the delivery chambers of a single printhead could negatively impact the clogging of the printhead during printing, according to previous initial testing. Therefore, separate printheads allocated to one specific solution were used to reduce this potential error. The allocated printheads had the same concentration of Histodenz or PEG respectively, in every delivery chamber of the printhead used for experiment. In an attempt to minimise the Histodenz exposure time for the cells, the mixing of cell suspension and test solution was performed exactly prior to printing. For printing, each printhead was exposed to the printing pressures presented

in Table 1.

**Table 1:** Printing pressures applied to the channels of the printhead during Biopixlar printing. The colours in brackets are referring to Figure 1 which illustrates the printhead.

| Microfluidic channels in printhead | Printing pressures [mbar] |
|---|---|
| Delivery channel (red) | 180 |
| Non-delivery channel (yellow, green & blue) | 8 |
| Internal vacuum / Switch (orange) | -50 |
| External vacuum / Recirculation (pink) | -150 |

### 3.4.1 Printing continuous lines (1)

The first printing strategy utilised was the semi-automatic mode, with printing procedure visualised in Figure 3. The solutions tested were 8 % [w/v] Histodenz, 12 % [w/v] Histodenz, 18 % [w/v] Histodenz and PEG 1.5 % [w/v] as control, which all contained hMSCs in standard concentration (800 000 hMSCs / 100 $\mu$l). The lines were automatically printed with the settings at a speed of 50 $\mu$m/s and a distance of 10 mm. At the end of a finished line, the printhead was moved manually in horizontal direction (approximately 500 $\mu$m), while still printing, to reach a starting point for the following line going in opposite direction to previously printed line. This procedure was repeated until the printing either, stopped due to clogging or because of the consumption of all the liquid loaded in the delivery chamber (25 $\mu$l). In the data analysis, cells were counted per region of interest with the surface area 0.25 mm$^2$ at determined distances (0, 2.5, 5, 7.5, 10, 15, 20, 30, 40, 50, 60, 70, 80, 90 mm) for each solution, with cut-off where the first replicate stopped printing.

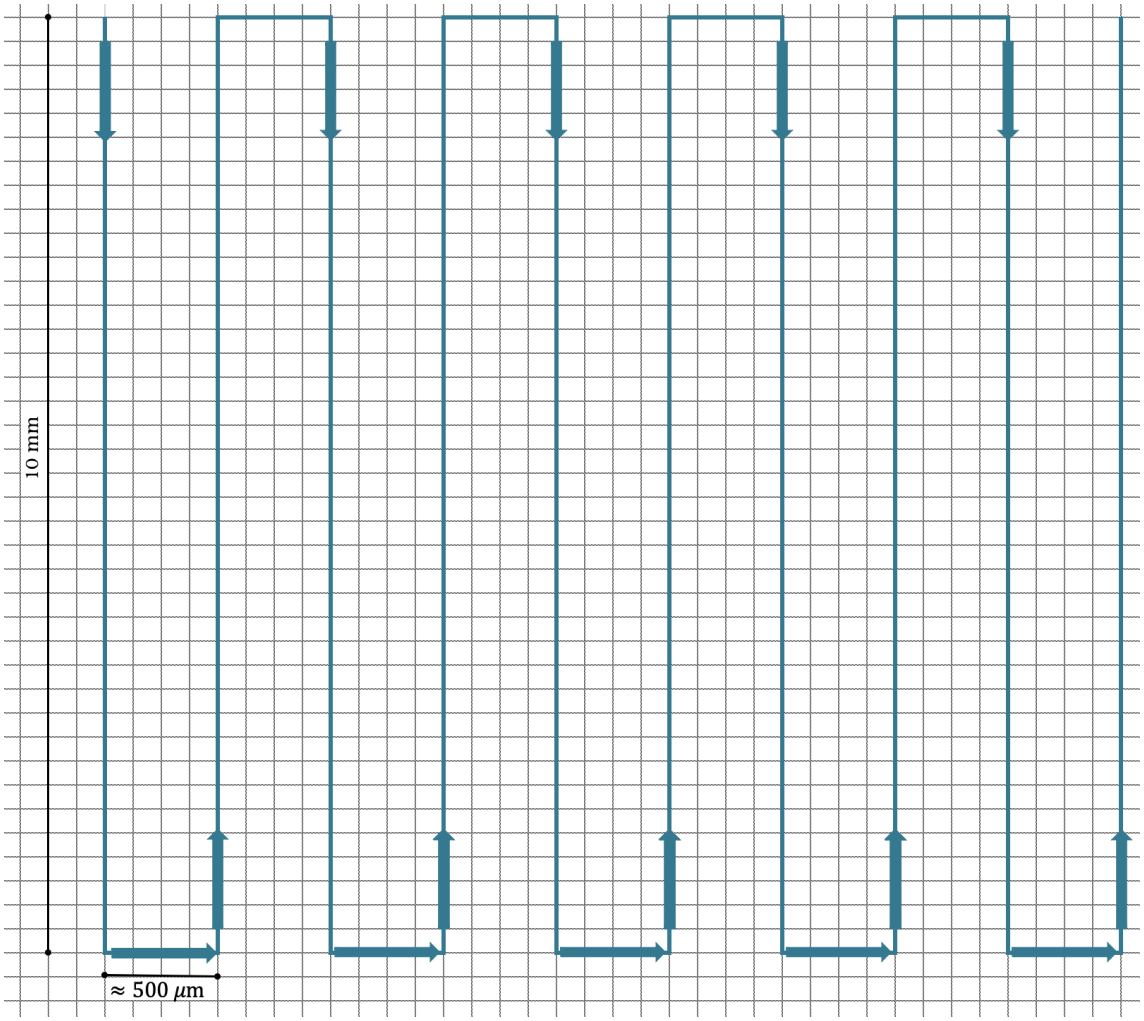


**Figure 3:** A schematic drawing of the printing procedure of printing strategy 1, performed in semi-automatic mode. Printing prolongs according to schematic until the cut-off point is reached. The printing distances are shown, with vertical lines of 10 mm and horizontal printing of approximately 500 $\mu$m.

### 3.4.2 Printing lines with intermediate breaks (2)

For the second printing strategy the automatic mode of the Biopixlar system was used, to print lines in pairs with intermediate breaks of three minutes, visualised in Figure 4. The script required for the automatic mode was created to print 1 mm long lines in pars of two. The first line was printed downwards and the second line upwards. When the printhead finalised the second line, it was programmed to wait for three minutes before starting the second pair of lines. The procedure was set to last for four pairs, although the script was extended to seven pairs after the first run. Equal printing pressures were used for all experimental rounds. The printing solutions used for this strategy were Histodenz with concentrations [w/v] 8 % and 12 % and PEG 1.5 % [w/v] as control. The printing was carried out until the complete number of pairs was printed or until the cut-off criteria were met. The cut-off criteria for this experiment were clogging of the tip. In data analysis, cell were counted pair-wise with a cut-off point defined as when more than a half of the

printed line in a pair was not printed.

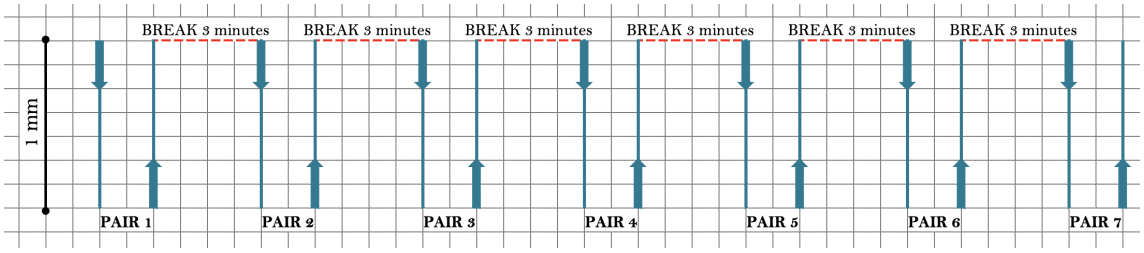


**Figure 4:** A schematic drawing of the printing procedure of printing strategy 2, performed in automatic mode. In total, seven pairs are displayed with lines of 1 mm each and the directions of intended printing are visualised with arrows. A printing break of three minutes separate each pair.

### 3.4.3 Viability staining of hMSCs and imaging

The printing was followed by an investigation of cell viability via live/dead staining assays using fluorescein diacetate (FDA, Sigma-Aldrich cat: F7378-5G) and propidium iodide (PI, Sigma-Aldrich cat: P4170). According to the FDA product protocol, live cells metabolise non-fluorescent FDA into fluorescein, which emits fluorescence in green spectrum. PI is instead capable of entering and staining nucleic acids in cells with non-intact membrane, which is stated in the product protocol. Therefore, the combined staining of these compounds result in green emission for the living cells and red emission for the dead cells. To allow cell count in image analysis, cells were stained with Hoechst dye (Fisher cat: H1399) which according to the product description binds to dsDNA. With established binding, the cells emit blue fluorescence from the nuclei. Stained samples were observed in 5X and 10X objectives of a fluorescence microscope (Zeiss Axiovert A1, Carl Zeiss, Germany) equipped with filters for emission detection (red, green and blue).

## 3.5 Image analysis

Images were obtained via the Carl Zeiss, ZEN software. The images were then opened and analysed in ImageJ2 image analysis and processing software. In the software, the full brightfield images were adjusted to increased brightness. Cell counts of DNA stained cells were performed in an automatic manner in ImageJ2 for printing strategy 2. Manual counting of cells in the images was performed if required and as control to the automatic counting. In addition, the images served as the basis for distance calculations performed for the printing strategies. For printing strategy 1, the long continuous lines were non-feasible to capture within one image. Therefore, manual cropping and tiling of the images was required. The data obtained from the images was analysed using Microsoft Excel.

# 4 Results

The results of the three experimental parts are described in this section. First, the viability and survivability of hMSCs are summarised in diagrams, which describe the measured effect of Histodenz solutions in terms of cell health. Secondly, the sedimentation of fluorescent particles in Histodenz solutions is visualised. Lastly, the results of printability with Histodenz solutions using different printing strategies are presented.

## 4.1 Histodenz impact on cell viability and survivability

In figure 5 the main results of the viability/survivability assays of hMSCs are presented, where the cells were exposed to a solution of either 8 %, 18 %, 30 % or 40 % [w/v] Histodenz. The remaining non-displayed data from the assays is included in Appendix C and serves as a methodology control. From Figure 5 (a) a slight decrease in hMSC viability can be observed with increase of Histodenz concentration. However, Histodenz 30 % [w/v] showed lower cell viability than Histodenz at 40 % [w/v] (62% versus 73 %) according to the MTT assay. The MTS assay was comparably stable and showed cell viability around 70-80 %. According to the standard error bars, the results of the MTS assay were the most reliable. Survivability of cells (24h after exposure to Histodenz, (Figure 3 (b)), indicates that Histodenz at higher concentrations possesses cytotoxic properties.

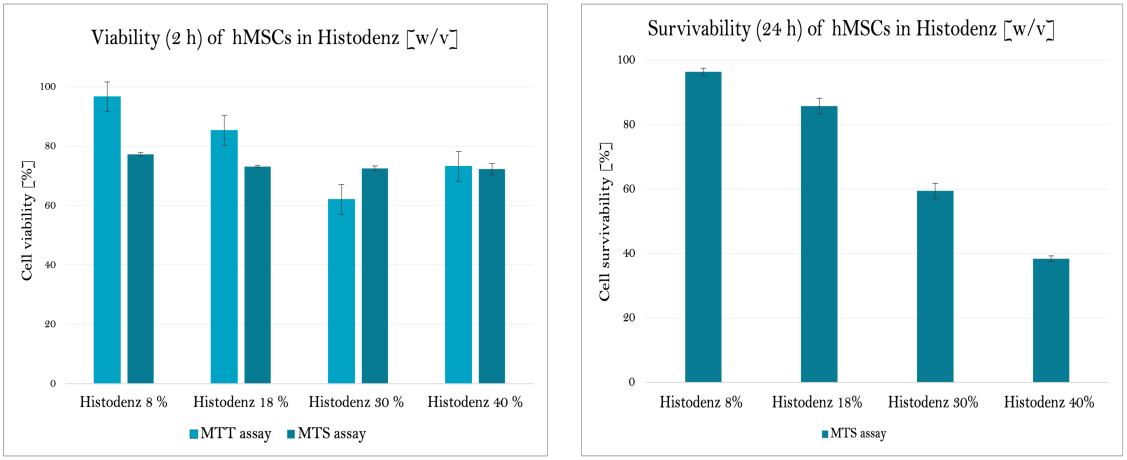


**(a)** **(b)**

**Figure 5:** Cell viability (a) and cell survivability (b) of hMSCs in 8 %, 18 %, 30 % and 40 % of Histodenz, respectively. The presented data show viable cells as percentage of the unexposed cell group. The cell viability results were measured by the two assays, MTT and MTS. Additionally, the standard errors bars are displayed.

The viability and survivability results were used to identify the initial experimental conditions, to work in a Histodenz concentration range where the cells were weakly affected by Histodenz. The results for the 8 % and 18 % [w/v] Histodenz solution were considered acceptable in terms of cell viability and cell survivability. Histodenz

solutions of 30 % and 40 % were determined to be unfeasible, as a large reduction in cell survivability was detected.

## 4.2 Sedimentation of fluorescent particles in Histodenz solution

Figure 6 shows the results of the three-hour sedimentation experiment, with fluorescent particles in different Histodenz concentrations. Control samples show that the particles in PBS alone completely settled to the bottom, while a phase separation close to the bottom occurred in PEG solution. For the Histodenz solutions, the lower percentages still sediments (up to 10 % [w/v]), while the higher percentages (10-30 % [w/v]) results in particles floating in the upper part of the Histodenz solution. The higher the concentration of Histodenz, the thinner the fluorescent band in the upper layers. The turning point where the particles go from sedimentation to floating appears to be in the range 10-14 % [w/v] of Histodenz solution.

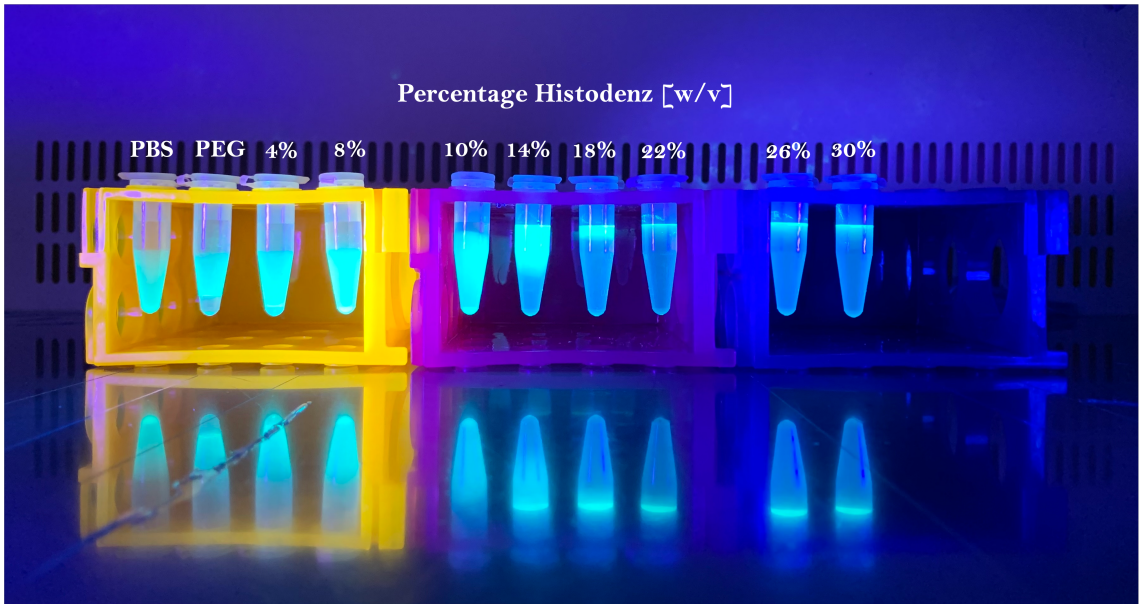


**Figure 6:** Equal volumes of fluorescent particles in different concentrations of Histodenz, ranging from the lowest 4 % to the highest 30 % [w/v]. The controls were PBS and PEG solution 1.5 % [w/v], respectively. Picture was taken 3 hours after the particles were left to sediment (1 x g).

The results in Figure 6 were used to find suitable Histodenz concentrations to test, in the hMSC printability experiments that followed. Because of differences in properties, such as particle size and density, the percentages found for fluorescent particles were not directly applicable for hMSCs, rather indicative. However, percentages lower than 8 % and higher than 18 % were further excluded due to the small probability of successful printing.

## 4.3 Printability experiments

The results of this section are divided into the different printing strategies used, printing continuous lines (1) and printing lines with intermediate breaks (2). The printability experiments covered the Histodenz concentrations 8 %, 12 % and 18 % [w/v] compared to the standard printing solution 1.5 % [w/v] PEG. Solutions were evaluated on printing distance, printed cell density and uniformity of printed lines.

### 4.3.1 Printability with printing strategy 1

In printing strategy 1, continuous lines of hMSCs were printed with solutions of PEG 1.5 %, Histodenz 8 % [w/v], Histodenz 12 % [w/v] and Histodenz 18 % [w/v], respectively. The 18 % [w/v] Histodenz solution was kept for the printability experiment, although the fluorescent particles were observed to float at the same concentration. The Histodenz concentration 18 % [w/v] was included to ensure that the concentration was not neglected solely by the particle experiment, as properties were different for the particles and the cells. Initial experiments confirmed that cells in the 18 % [w/v] Histodenz solution float similarly to the beads, whereof the solution was further excluded.

In Figure 7, representative pictures of the printed distances of each solution are presented. The distance of PEG solution 1.5 % [w/v] is seen to be shorter than the Histodenz solutions of 8 % and 12 % [w/v]. With respect to uniformity of intended shape (line), the PEG solution (a) is unevenly printed compared to the Histodenz solution (b-c). An unevenness is also noticeable in Figure 7 (c), at the end of the line.

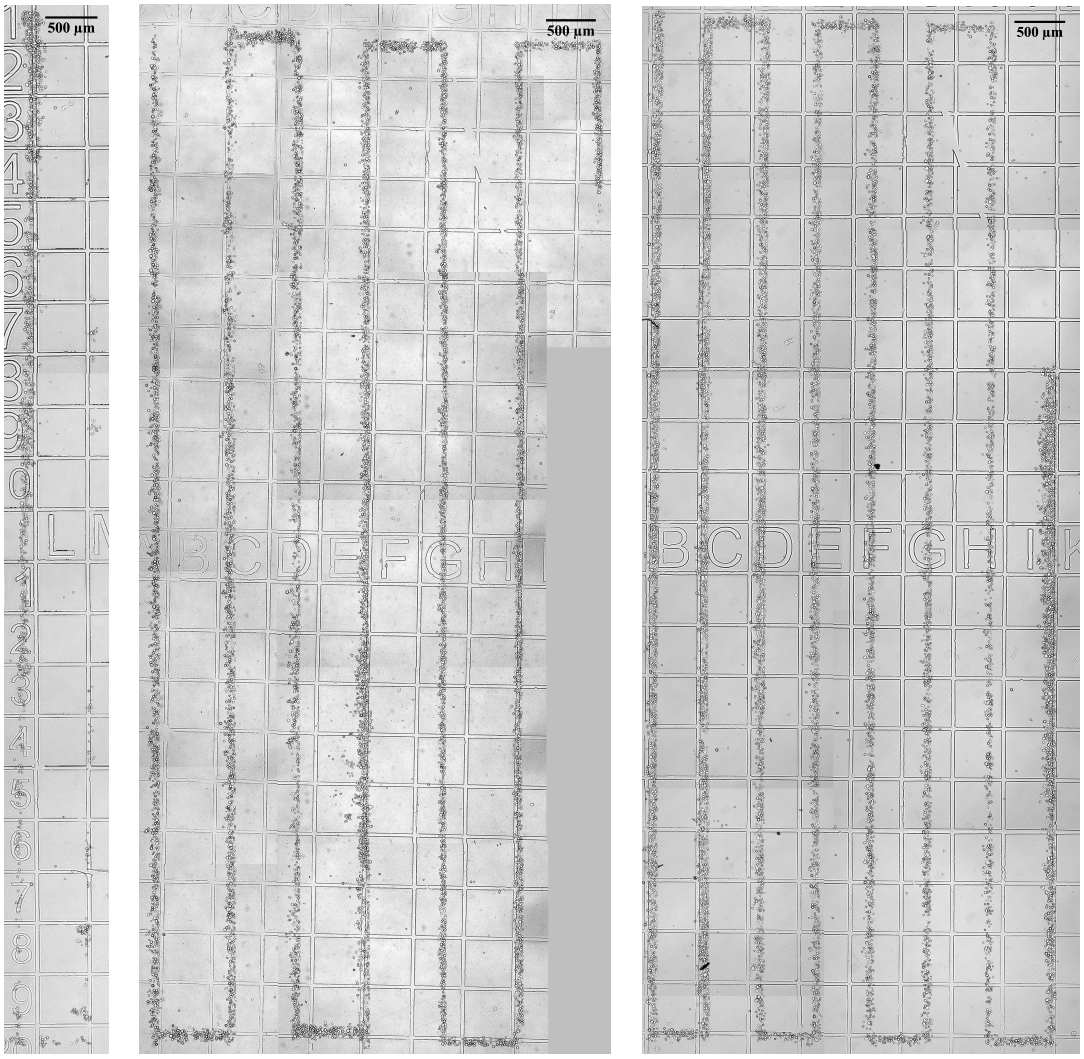


**(a)** Printed with PEG solution 1.5 %

**(b)** Printed with Histodenz solution 8 %

**(c)** Printed with Histodenz solution 12 %

**Figure 7:** The figure displays representative images of hMSCs printed continuously in long lines of 10 mm with PEG 1.5 %, Histodenz 8 % and 12 % [w/v] solutions, respectively. Horizontal printing was performed in between the long lines to achieve a new starting point without interrupting cell injection. PEG solution 1.5 % [w/v] reached a comparably short distance before clogging, while longer distances could be obtained using the Histodenz solutions 8 % and 12 % [w/v].

The quantification of the printing distance with each solution is summarised in Figure 8, where on average 14, 68 and 85 mm long lines were printed, respectively for PEG 1.5 %, Histodenz 8 % and 12 % [w/v] solutions. The Histodenz solutions enable longer printing distances compared to the PEG solution.

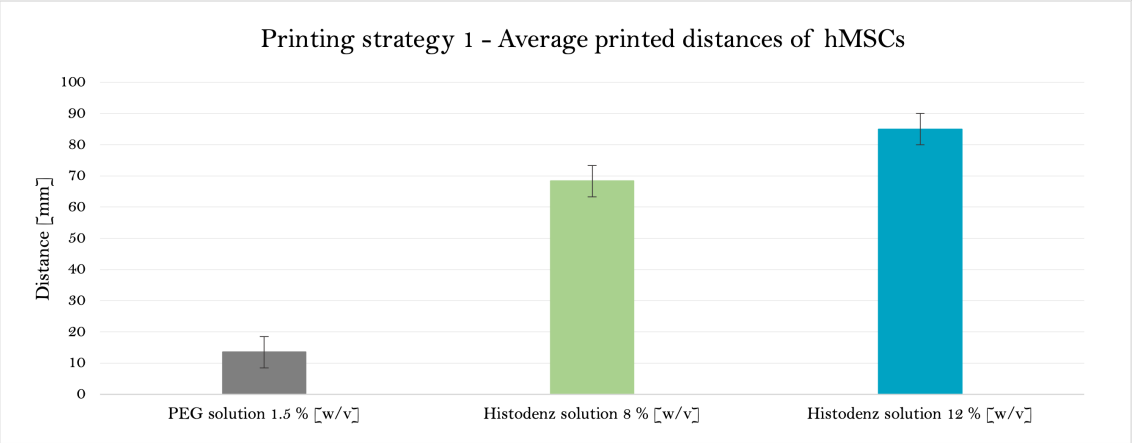


**Figure 8:** The average printed distances of hMSCs in PEG 1.5 %, Histodenz 8 % and Histodenz 12 % [w/v] solution, were 14, 68 and 85 mm, respectively, using printing strategy 1. The standard error bars represent the variation in the results of each solution, N=3.

The other important aspect, cell density (here number of cells per region of interest, which was defined as a grid square of the cell dish with the surface area 0.25 $mm^2$), was evaluated to assess printing quality. The cell count was averaged for each solution and presented in Figure 9 below. The dash-dotted line, that follows the solid line, represents data that have less than three data points (cut-off point), therefore statistical analysis could not be performed, yet they are included to indicate the trend. Thus, the dash-dotted lines describe where at least one printhead, for each solution, had stopped printing. According to the observations, the PEG solution produces lines with a high cell count immediately after the initiation of printing. The start was followed by a steep drop, observed in cell density on the surface, until the first printheads clogged in the interval of 10-15 mm. Both Histodenz solutions resulted in lower cell density in the beginning. The 8 % [w/v] gave an increase in cell count during the first 5 mm (approximately 50 % increase) before a declining trend is observed for the next 45 mm printing distance, reaching similar cell density as at the beginning of the print (approximately 50 cells per 0.25 $mm^2$). The first clogging of the tip (cut-off point) is observed at a distance between 50 and 60 mm from the printing start position. Histodenz solution 12 % [w/v] displays a relatively steady declining trend, similar to that of 8 % [w/v], although without the increase in the beginning. Cell count slowly droped by approximately 30 % (from 70 to 50 cells per region of interest) in a distance of 70 mm. Remarkable is the final peak of all print replicates, where a sudden increase of cell count is observed (almost 100 % increase over 10 mm distance), followed by abrupt print end. Cell recirculation stopped for all three replicates in the 80-90 mm interval.

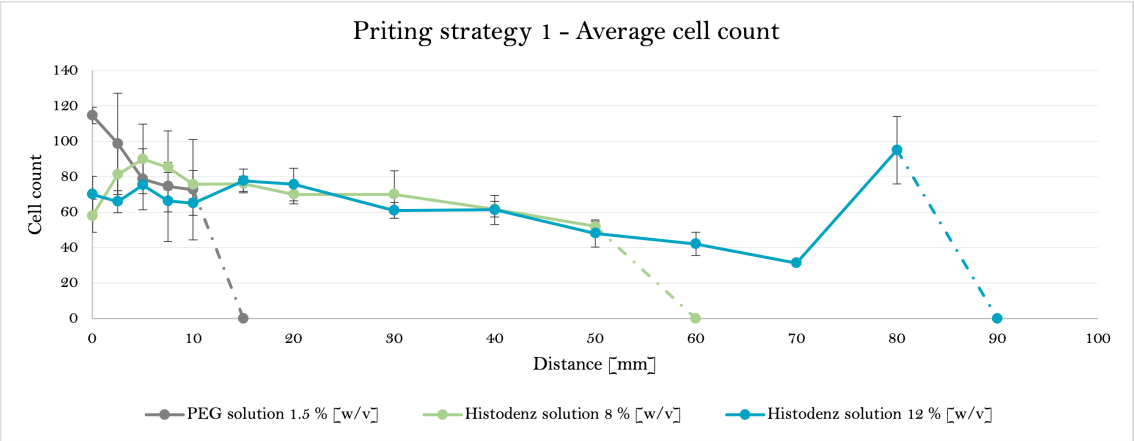


**Figure 9:** The graph display obtained results for cell count (cells per 0.25 $mm^2$) with printing strategy 1, at determined distances for the solutions PEG 1.5 % [w/v], Histodenz 8 % [w/v] and Histodenz 12 % [w/v]. The standard error bars show the variation in cell count, N=3 for each solution. The dashed-dotted lines represent data points where one or several printing experiments reached cut-off point and data had less than three repeats, yet shown on the graph to indicate the trend.

### 4.3.2 Printability with printing strategy 2

The initial results from the printing strategy with intermediate breaks are visualised in Figure 10 below. Tested concentrations of Histodenz were 8 % and 12 % [w/v], while PEG solution 1.5 % [w/v] was used as control. The pairs of lines, each line of 1 mm, were printed with three minutes intermediate breaks. The experiment included a maximum of four pair of lines for each solution, which all are displayed in the figure. In Figure 10 (a) the lines printed with PEG solution 1.5 % [w/v] are generally thick and uneven for all the time points (0, 3, 6 and 9 minutes after printing initiation). Additionally, the maximum printing time with PEG solution 1.5 % [w/v], where lines were printed, was on average six minutes. Figure 10 (b) presents data of the 8 % [w/v] Histodenz solution, where thinner printed lines for the first three pairs can be observed, in comparison to printed lines with PEG solution 1.5 % [w/v]. In addition, cells can be detected at nine minutes time point, however, not in the shape of lines as intended by this experiment. Lastly, Figure 10 (c) presents the result for the 12 % [w/v] Histodenz solution. With the higher Histodenz percentage, all four pairs were printed and appeared to be fairly uniform in shape, as intended.

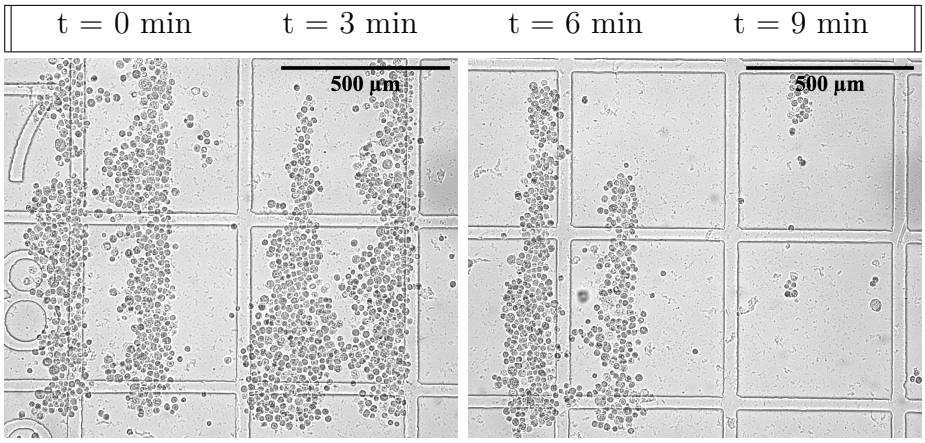


**(a)** Printed hMSCs with 1.5 % PEG solution

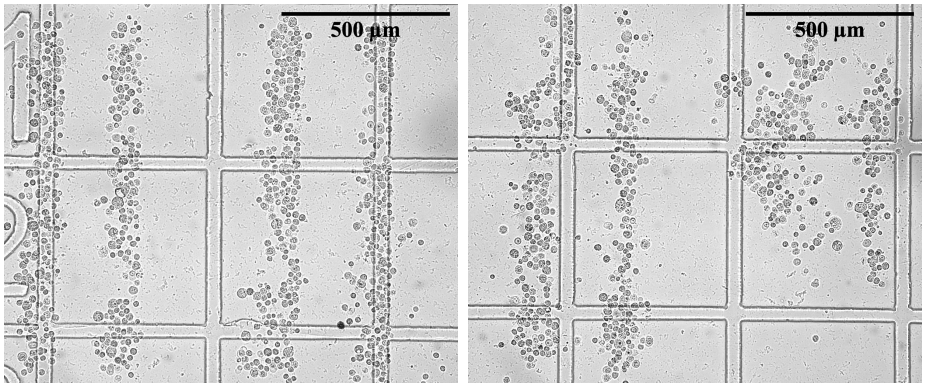


**(b)** Printed hMSCs with 8% Histodenz solution

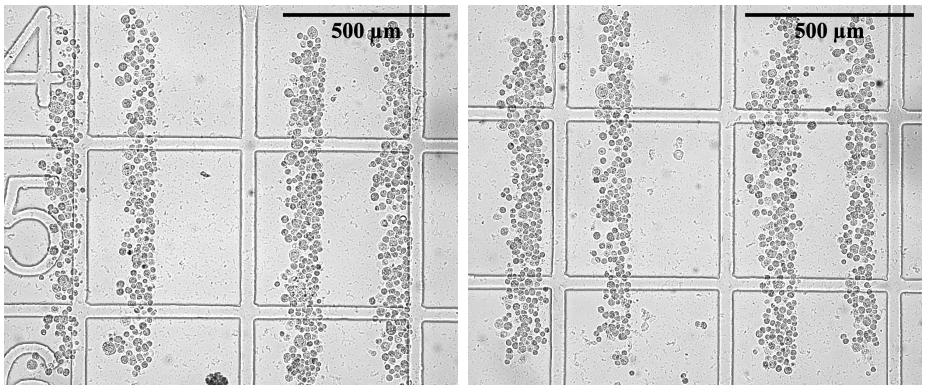


**(c)** Printed hMSCs with 12% Histodenz solution

**Figure 10:** Images displaying the results from printing strategy (2), where (a) hMSCs in PEG solution 1.5 % [w/v], (b) 8% Histodenz solution [w/v] and (c) 12% Histodenz solution [w/v], were printed in 1 mm long lines, respectively. Each pair of lines were printed with a three minutes intermediate break.

For the initial results, presented in Figure 10, a cell count (here cells per pair of lines) was performed to assess the cell density printed with the different solutions. The purpose was to also analyse the printing efficiency, in terms of cell amount printed to the surface at each time point. Printed cell densities obtained for each solution are presented in Figure 11. As can be seen from the figure, the density of

cells suspended in PEG solution 1.5 % [w/v], decreases over time. Although the first three pairs of hMSCs printed in PEG solution 1.5 % [w/v] were successfully printed, in terms of complete lines (see Figure 10 a), the cell count at later time points (6 and 9 minutes) indicates an instant decrease in the printability performance. On the other hand, both Histodenz solutions, show more stable printability, based on the cell count in comparison to the PEG solution. The cell count of 8 % [w/v] Histodenz solution starts to decrease after six minutes, however, not as steep as PEG solution 1.5 % [w/v]. The most prominent result for cell count is the Histodenz solution of 12 % [w/v], where no reduction was detected over the duration of the experiment.

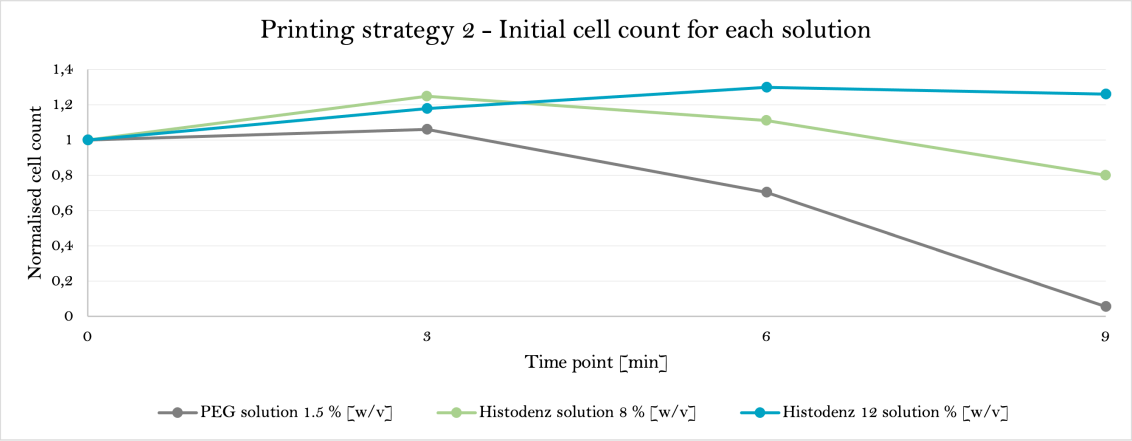


**Figure 11:** The graph presents the normalised cell count par pair of lines (hMSCs) with respect to the printing initiation of each solution (t = 0 min). The three solutions tested were PEG solution 1.5 % and Histodenz solutions of 8 % and 12 % [w/v]. The counts were based on the cells shown in Figure 10 above measured pairwise.

As the 12 % [w/v] Histodenz solution had shown to be the better alternative in the initial results of printing strategy 2, among other tested Histodenz concentrations (Figure 11), it was decided to proceed with that solution for further analyses. Using the same printing strategy, an extended experiment in terms of printing duration was carried out, to analyse the capacity of Histodenz solution 12 % [w/v].

The data for the cell count (here cells per pair) of the extended experiment is shown in Figure 12. In total seven pairs of lines were printed at the interval of 3 minutes (time points 0 to 18). As previously explained, the dashed-dotted line represents the interval wherein one or more printhead were clogged therefore cut-off point was reached. The cut-off point was defined as the time point where more than a half of a printed line was not printed (counting was performed in units of 0.5 mm). In Figure 12, the PEG solution was high in cell count initially with a decreasing trend in the following pair. After the second pair, clogging of the printheads was observed. A lower initial printed cell number was observed when printing with Histodenz 12 % [w/v], however it remained quite stable, only slowly decreasing in printed cell density by 25 % over 18 min experimental run. The use of Histodenz solution enabled printing of all seven pairs (18 min). Lastly, the standard error bars explain low variability in cell count for the Histodenz solution, N=6, compared to the PEG solution, N=5.

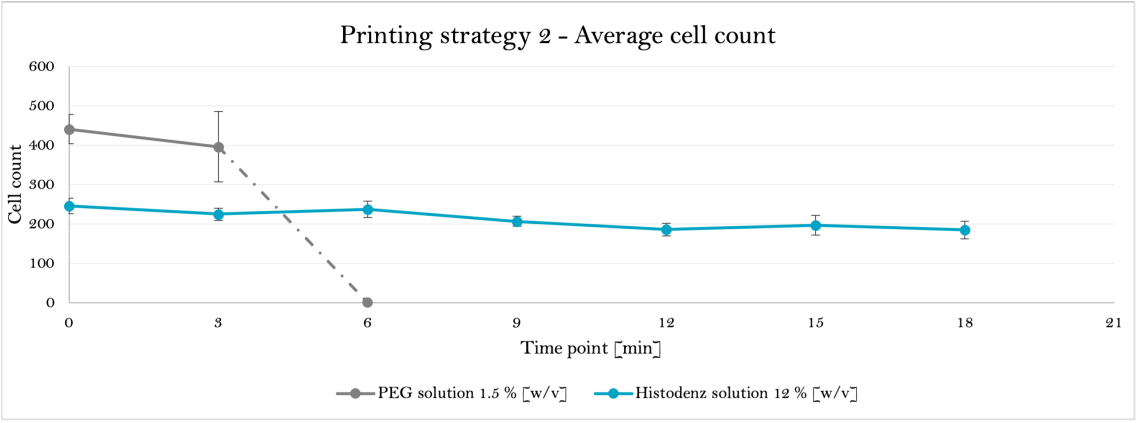


**Figure 12:** The graph shows the average cell count (cells per pair of lines) obtained in the printing strategy 2 where pairs of lines was printed with intermediate wait time of three minutes. Solutions tested were PEG solution 1.5 % [w/v] (N=5) and Histodenz solution 12 % [w/v] (N=6) respectively. The dashed-dotted line represents data, where cut-off point was reached, i.e. clogging of the printhead was detected in one or more experimental repeats. The cut-off point was defined as the time point where more than a half a line in a pair was not printed.

The distance obtained for the solutions using extended printing strategy 2 was measured in the number of pairs, presented in Figure 13. The number of pairs were counted in 0.5 mm units, corresponding to the cut-off point. In Figure 13, the average number of pairs printed with each solution are visualised. For PEG solution 1.5 % [w/v] (N=5) the average number of printed pairs were three, while seven printed pairs in average were reached with Histodenz solution 12 % [w/v] (N=6).

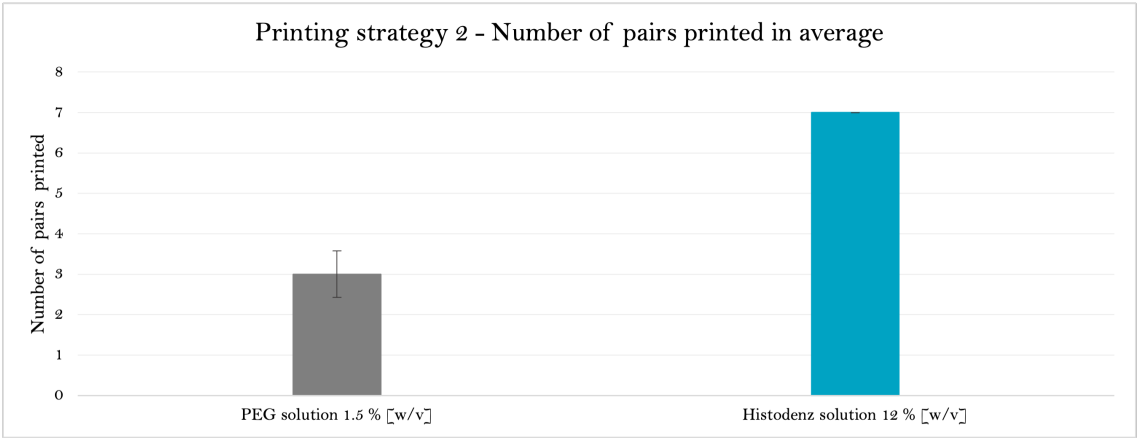


**Figure 13:** The figure shows the number of pairs printed in average for the solutions PEG 1.5 % and Histodenz 12 % [w/v]. The pairs were counted in units of 0.5 mm of a line. The cut-off was set to when a length of 0.5 mm was no longer fulfilled, equally to when a half of a line in the pair was missing. The standard error bars indicate the data distribution.

### 4.3.3 Viability control

In a concluding step, a viability control of printed hMSCs was performed to investigate any impact from the printing procedure and Histodenz solution effect. The control was based on one set of images (a-b) from printing strategy 2, displayed in Figure 14. Representative images of Histodenz solution 12 % [w/v] and PEG solution 1.5 % [w/v] in experimental runs are shown in Figure 14 (a-b). Images (c-d), presents the PI staining for identification of dead cells for both solutions. Lastly the FDA staining of the cells, printed with the different solutions, are visualised in (e-f). The viability of hMSCs printed with Histodenz solution 12 % [w/v] was calculated to 66 %, while a 70 % viability was observed for PEG solution 1.5 % [w/v] printing.

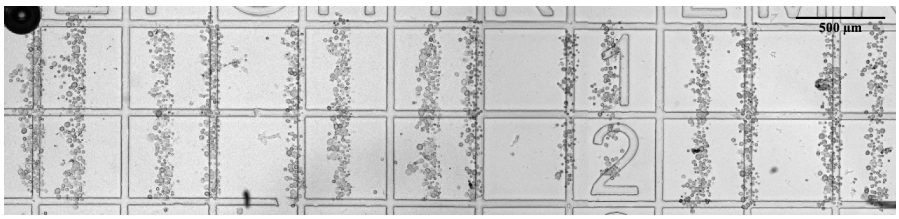


**(a)** hMCs printed with Histodenz solution

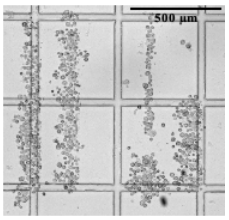


**(b)** hMCs printed with PEG solution

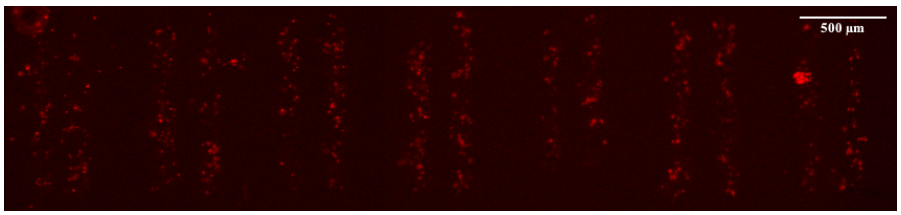


**(c)** hMCs printed with Histodenz solution, visible PI staining

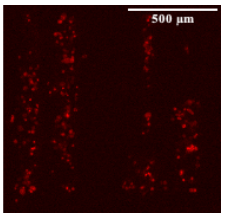


**(d)** hMCs printed with PEG solution, visible PI staining

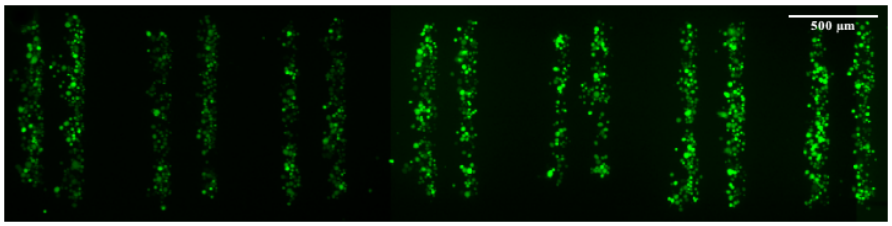


**(e)** hMCs printed with Histodenz solution, visible FDA staining

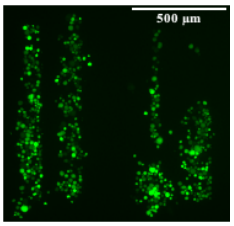


**(f)** hMCs printed with PEG solution, visible FDA staining

**Figure 14:** Representative images of hMSCs printed with Histodenz solution 12 % [w/v] (a, c, e) and PEG solution 1.5 % [w/v] (b, d, f) for cell viability control after printing. The PI staining visualises the dead cells in (c-d), while the FDA visualises the viable cells in (e-f).

# 5 Discussion

Printing viable cells is a core foundation in bioprinting. Therefore, viability assays (MTT/MTS) were conducted (Figure 2), where seeded cells were exposed to Histodenz solutions (8 %, 18 %, 30 % and 40 %), to assess if Histodenz impact cell health. For the two lowest concentrations of Histodenz tested (8 % and 18 % [w/v]), an average viability (based on the two lowest concentrations of both assays, total of four measurements) of approximately 83 % and a survivability (based on the two lowest concentrations) of 91 % were registered. In general, a cell viability higher than 83 % would be preferable, but the experimental setup included the Histodenz exposure time of 3h to mimic maximum possible, yet unlikely, printing time. Therefore, it was expected that such viability represents a worst case scenario, that can be expected from cell printing experiments and . A preferable improvement of the experimental setup would, however, be if the standard printing solution PEG was included in the assays as an additional control, for viability evaluation under equal conditions. Further, since the printing process could influence viability, studies of viability of printed hMSCs were performed, see Figure 14. The cell viability obtained for printed hMSCs was 66 %, that was lower than expected from initial cell viability experiments and especially low in comparison to 95 % feasible with current printing solution (PEG). However, this experimental setup was designed to be performed in PBS instead of hMSC medium, which adds additional stress to the cells. Still, PBS was chosen since the solution is usually used in initial tests, when cell dishes are not aimed to be kept for longer monitoring. An improvement would probably be seen if a viability control were performed after printing in media.

In order to fast track finding a relevant concentration interval of Histodenz, a sedimentation experiment with fluorescent beads was performed. By the experimental setup, multiple Histodenz concentrations could be tested for suitability in Biopixlar printing even prior to actual printing. The fluorescent particles were left to sediment (in PBS, PEG 1.5 %, 4 %, 8 %, 10 %, 14 %, 18 %, 22 %, 26 % and 30 % [w/v]) by the force of gravity, to mimic cell sedimentation in printhead chambers. The extreme case of maximum printing time (3h) was used for sedimentation experiment and was equal to the exposure times in the MTT/MTS assays. Thus, Figure 6 mimicked a situation of sedimentation similarly to cell sedimentation in the printhead chamber after an entire printing session. However, in a regular printing procedure the particles or cells will be continuously removed from the bottom of the printhead delivery chamber during a 3h printing session (channels connect to the chambers in the bottom), which was not feasible to mimic in this experimental set up. Thus, it is important to note that the sedimentation gradient shown in Figure 6 would likely appear differently in a printing procedure, showing less fluorescence at the bottom part of the tubes (PBS, PEG 1.5 %, 4 %, 8 %, 10 % [w/v]). In a natural printing procedure the suitable solution enables sedimentation occurring at a rate slower than in PEG (to improve printability), while more rapidly than 3 hours (to maintain printing function). The result of particle sedimentation was only indicative although found fairly applicable for hMSCs. For instance, it is possible that cells with higher density and smaller single-cell diameters, which imply faster sedimentation rates, require higher percentages of Histodenz as printing solution.

For printing strategy 1, where continuous long lines of hMSCs where printed, the most promising results in terms of printability were found for Histodenz solution 12 % [w/v]. However, the solution had decreased uniformity at the end of the continuous line (in Figure 7). The increased cell density towards the end of the line is probably a consequence of the limited volume loaded into the delivery chamber (25 $\mu$m), as the chamber was almost entirely emptied for all replicates. Appendix D Figure 3, displays an example of such a printhead which printed increased cell density before it stopped printing. It can be seen that its delivery chamber was almost emptied during the printing. Additionally, Appendix D Figure 4 presents an example of when the increase in cell density was followed by the release of air from the printhead, due to an entirely emptied delivery chamber. Injection of air (generation of air bubble) is indicative to full consumption of chamber solution, whereas cessation of print without observing air bubbles is caused most likely by printhead clogging. It is possible that cells, in an almost emptied delivery chamber, get exposed to higher shear forces against the chamber surface due to the low remaining liquid, making them more prone to aggregate. Cell aggregates large enough to clog the printhead may form toward the end, before the delivery chamber gets depleted. Due to the uniformity issue at the end of the continuous line, printing distances as far as 85 mm (Figure 8) with printing strategy 1 should be avoided in high-precision printing. Instead, it is advisable not to exceed a distance of 70 mm (Figure 9) as the data indicates decent uniformity, although a decrease in cell density on the surface is observed. For more comprehensive understanding of results, the data can be converted to the printing duration. Under current experimental setup (print speed, cell concentration, printing pressures) successful printing was possible for 23.3 minutes using Histodenz 12 % [w/v]. These results show a substantial increase in print time compared to the PEG solution, with a possible print time of only 3.3 minutes, indicating a massive increase by 600 %. The possibility of extended printing by switching delivery chamber was not tested due to overfill of the recirculation waste chambers, see Appendix D Figure 3 (7-8). Furthermore, switching to a new delivery chamber after 23.3 minutes would not necessarily work, since the cells then had an initial time to sediment without continuous removal from the bottom upon printing. A higher cell density at the bottom of the chamber would make the printhead more prone to clogging.

Similarly for printing strategy 2, where pairs of lines of hMSCs where printed with intermediate breaks, the Histodenz solution 12 % [w/v] was the most promising, already in the initial experiment with four pairs. According to Figure 10, uniformity of printed shape was in favour for hMSCs printed with Histodenz 12 % [w/v]. In the extended experiment of seven pairs, all pairs were printed successfully with the Histodenz solution. Actually, since all the replicates finalised the last pair (described by the standard error bar of value 0 in Figure 13), the limit of number of pairs feasible to print with Histodenz solution 12 % [w/v] seems to be beyond seven. However, limited printhead recirculation waste chambers volume defined the maximum duration of the printing experiment under current pressure settings (see Table 1). When printing with Histodenz solution compared to PEG solution, the average numbers of pairs printed is increased with 4 pairs (Figure 13). The printing time difference (Figure 12) between the Histodenz solution 12 % [w/v] (18 minutes) and PEG (3

minutes) is 500 %. Along with a stable cell density throughout the printing round with intermediate pauses, such Histodenz solution 12 % [w/v] performance can be considered as a superior candidate for future applications.

It is important to address the possible sources of errors in obtaining these results. Automatic hMSCs cell counting during the analysis step, could result in under-counting in areas of high cell density. Image analysis software, in areas of higher cell density, could not separate single cells in cell clusters and aggregates, often merging and counting such structures as one cell. However, for certain images with high cell density, cells in some areas had to be merged to more accurately represent the original picture. Therefore, there is a risk that the cell count values are lower than actual. To address this issue manual cell counting was performed in a smaller area of each image and differences were minor. Furthermore, human error may have influenced control counting, thus, the counted values for each solution should be viewed as relative to the other solutions rather than precise. Similar reasoning applies to the images in Figure 14, where the thresholds for cell count were difficult to determine mainly due to background.

In summary, out of all of the Histodenz solutions tested ( 8 %, 12 % and 18 % [w/v]), the solution of 12 % [w/v] performed best in all evaluation points of both printing strategies. Histodenz solution of 12 % has drastically improved printability, confirmed by printing longer distances with uniform cell density. As a consequence, the printing time has drastically increased, reducing the time wasted to resuspend the cells in the chambers when cells sediment and print density reduces (standard procedure with current PEG solution). Referring to the interval found for theoretical single-cell densities, hMSCs seem to have an average single-cell density slightly higher than 1.06g/cm$^3$ of Histodenz solution 12 % [w/v]. The indication of the single-cell density value is based on the sedimentation of hMSCs in Histodenz solution 12 % [w/v], shown by the ability to print cells. The single-cell densities, 1.04 g/cm$^3$ (8 % Histodenz) and 1.09 g/cm$^3$ (18 % Histodenz), were excluded and the narrow interval ($\pm$0.03 g/cm$^3$) indicate on complexity in standardising one concentration for all cell types. Future work is required to expand the area of use of Histodenz [w/v] for other cell types, yet this work defined the concentration range where future work should be conducted.

## 5.1 Future work

Additional work remains to be conducted to ensure cell health for Histodenz-printed hMSCs. Preferably, multiple dishes containing printed cells in media, instead of in PBS, can be analysed with FDA/PI staining. Thus, the viability results will better reflect the printing performance obtainable using Histodenz. Furthermore, Histodenz 12 % [w/v] proved to be a suitable concentration for printing hMSCs with Biopixlar, however, parameter optimisation remains for future work. It is possible that minor adjustments in percentage units of Histodenz concentration would improve the printing or cell viability. Additionally, a change of the hMSC concentration for printing would be desired, as the current concentration is optimised for PEG printing (based on previous experimental work). Changing the cell concentration is

related to further evaluation of printhead clogging, as the printhead might be more prone to clogging with higher cell concentrations. Lastly, the Histodenz solution should also be tested in manual mode of Biopixlar, as printability using Histodenz with this printing mode has not yet been evaluated.

Future work is also required to ensure cell health for other cell lines printed with Histodenz solution. Cell health is important to control, as there might be cell lines having higher sensitivity towards Histodenz. Additionally, more cell types need to be tested, as sizes and densities of the different cells can differ implying optimal Histodenz concentrations to be specific for a certain cell type. The work conducted during this thesis has established a route to determine such a concentration, wherefore future work could be performed in shorter time and with less efforts. For instance, the suitable Histodenz concentration for hMSCs was consistently performing better than the other concentrations tested regardless of printing strategy. Therefore, future experiments could be conducted utilising only one of the printing strategies tested.

In addition, current printing strategies and pressures were limited by waste chambers filling to the maximum volume. Therefore, future attempts to extend the possible printing time should involve adjusting the printing pressures. The focus will be to find the optimal balance in pressures, where the liquid volume getting aspirated back in the printhead is minimised while a desired recirculation zone is still maintained. In a situation with optimal pressures, it will take longer time for the waste chambers to be filled by the aspirated liquid and a possibility of extended printing duration arises.

# 6 Conclusion

This project has evaluated the use of Histodenz solution for optimising Biopixlar printing protocols with regards to printability (impact on cell viability, uniformity of printed shape, cell deposition densities and printing duration). Viability of hMSCs exposed to Histodenz showed lower viability (66 % - 80 %) compared to the standard PEG solution (previously tested to be approximately 95 %). Thus, extended tests of cell viability are further needed for the Histodenz solutions to be listed in a standard operational protocol for daily usage, and additional optimisations could contribute to increased viability. In the evaluation of uniformity of printed shape, PEG solution showed some limitations compared to the Histodenz concentrations of 8 % and 12 % [w/v]. The Histodenz solution 12 % [w/v] showed improved uniformity when printing pairs of lines with intermediate breaks, compared with the uniformity obtained printing with PEG solution. However, in the strategy of printing continuous long lines, unevenness (in the shape of the line) was observed towards the end of the printing run. This could be explained by an almost emptied delivery chamber and a recommendation would be to avoid printing longer than approximately 23 minutes of continuous printing. The lines printed with Histodenz solution 8 % [w/v] was not uniform for all pairs of lines (printing with strategy 2), in addition printing continuous long lines (printing strategy 1) was less efficient with Histodenz of 8 % [w/v] than the 12 % [w/v]. Cells in Histodenz solution of 12 % [w/v] were successfully printed in seven pairs of lines in printing strategy 2, corresponding to 18 minutes, compared to 3 minutes observed with the PEG solution. Furthermore, a continuous long line of 70 mm were successfully printed using Histodenz solution 12 % [w/v], compared to the 10 mm obtained with PEG. These results imply, that substituting PEG with Histodenz 12 % [w/v], can increase printing efficiency (distance wise) up to 500-600 %. According to the cell counts performed, Histodenz 12 % [w/v] showed the least declining trend as well as best pattern uniformity between the measurements. Therefore, it can be concluded that Histodenz 12 % [w/v] improves printability in three out of four aspects (uniformity of printed shape, cell deposition densities and printing duration), where the fourth aspect (cell viability) needs additional investigation and optimisation. Even at this stage, Histodenz solution performance can be considered superior over PEG solution. Additional optimisations on increasing viability of cells upon exposure to Histodenz with high probability will substitute the currently used PEG solution in tissue patterning protocols.

# References


[1] N Shahrubudin, T C Lee, and R Ramlan. "An Overview on 3D Printing Technology: Technological, Materials, and Applications". In: *Procedia Manufacturing* 35 (2019), pp. 1286–1296. ISSN: 2351-9789. DOI: 10.1016/j.promfg.2019.06.089.

[2] Sean V Murphy and Anthony Atala. "3D bioprinting of tissues and organs". In: *Nature Biotechnology* 32.8 (2014), pp. 773–785. ISSN: 1546-1696. DOI: 10.1038/nbt.2958.

[3] Ashley N Leberfinger et al. "Bioprinting functional tissues". In: *Acta Biomaterialia* 95 (2019), pp. 32–49. ISSN: 1742-7061. DOI: 10.1016/j.actbio.2019.01.009.

[4] Selwa Boularaoui et al. "An overview of extrusion-based bioprinting with a focus on induced shear stress and its effect on cell viability". In: *Bioprinting* 20 (2020). ISSN: 2405-8866. DOI: 10.1016/j.bprint.2020.e00093.

[5] Silvia Santoni et al. *3D bioprinting: current status and trends—a guide to the literature and industrial practice*. Jan. 2022. DOI: 10.1007/s42242-021-00165-0.

[6] Pallab Datta et al. "Essential steps in bioprinting: From pre- to post-bioprinting". In: *Biotechnology Advances* 36.5 (2018), pp. 1481–1504. ISSN: 0734-9750. DOI: 10.1016/j.biotechadv.2018.06.003.

[7] Hyeong Jin Lee et al. *Recent cell printing systems for tissue engineering*. 2017. DOI: 10.18063/IJB.2017.01.004.

[8] *BIOPIXLAR WILL BE LAUNCHED THE 6TH OF NOVEMBER 2019*. URL: https://fluicell.com/biopixlar-will-be-launched-the-6th-of-november-2019/.

[9] *BIOPIXLAR® 3D SINGLE-CELL BIOPRINTING*. URL: https://fluicell.com/products-fluicell/biopixlarplatform/.

[10] Anh Tong et al. *Review of Low-Cost 3D Bioprinters: State of the Market and Observed Future Trends*. Aug. 2021. DOI: 10.1177/24726303211020297.

[11] Ibrahim T Ozbolat, Kazim K Moncal, and Hemanth Gudapati. "Evaluation of bioprinter technologies". In: *Additive Manufacturing* 13 (2017), pp. 179–200. ISSN: 2214-8604. DOI: 10.1016/j.addma.2016.10.003.

[12] Lukas Wenger, Svenja Strauß, and Jürgen Hubbuch. "Automated and dynamic extrusion pressure adjustment based on real-time flow rate measurements for precise ink dispensing in 3D bioprinting". In: *Bioprinting* 28 (2022). ISSN: 2405-8866. DOI: 10.1016/j.bprint.2022.e00229.

[13] Zhengyi Zhang et al. "Evaluation of bioink printability for bioprinting applications". In: *Applied Physics Reviews* 5.4 (Dec. 2018). ISSN: 1931-9401. DOI: 10.1063/1.5053979.

[14] Tao Zhang et al. "Bioink design for extrusion-based bioprinting". In: *Applied Materials Today* 25 (2021). ISSN: 2352-9407. DOI: 10.1016/j.apmt.2021.101227.

[15] Srikanthan Ramesh et al. "Extrusion bioprinting: Recent progress, challenges, and future opportunities". In: *Bioprinting* 21 (2021). ISSN: 2405-8866. DOI: 10.1016/j.bprint.2020.e00116.

[16] Alexander D Graham et al. “High-Resolution Patterned Cellular Constructs by Droplet-Based 3D Printing”. In: *Scientific Reports* 7.1 (2017). ISSN: 2045-2322. DOI: 10.1038/s41598-017-06358-x.

[17] Ashley N Leberfinger et al. “Concise Review: Bioprinting of Stem Cells for Transplantable Tissue Fabrication”. In: *Stem Cells Translational Medicine* 6.10 (Oct. 2017), pp. 1940–1948. ISSN: 2157-6564. DOI: 10.1002/sctm.17-0148.

[18] Tao Xu et al. “Inkjet printing of viable mammalian cells”. In: *Biomaterials* 26.1 (2005), pp. 93–99. ISSN: 0142-9612. DOI: 10.1016/j.biomaterials.2004.04.011.

[19] Hemanth Gudapati, Madhuri Dey, and Ibrahim Ozbolat. “A comprehensive review on droplet-based bioprinting: Past, present and future”. In: *Biomaterials* 102 (2016), pp. 20–42. ISSN: 0142-9612. DOI: 10.1016/j.biomaterials.2016.06.012.

[20] Pranabesh Sasmal et al. “3D bioprinting for modelling vasculature”. In: *Microphysiological Systems* 1 (2018). DOI: 10.21037/mps.2018.10.02.

[21] Haowei Yang et al. “Laser-based bioprinting for multilayer cell patterning in tissue engineering and cancer research”. In: *Essays in Biochemistry* 65.3 (Aug. 2021), pp. 409–416. ISSN: 0071-1365. DOI: 10.1042/EBC20200093.

[22] Chaoran Dou et al. “A State-of-the-Art Review of Laser-Assisted Bioprinting and its Future Research Trends”. In: *ChemBioEng Reviews* 8.5 (Oct. 2021), pp. 517–534. ISSN: 2196-9744. DOI: 10.1002/cben.202000037.

[23] Jason A Barron et al. “Application of laser printing to mammalian cells”. In: *Thin Solid Films* 453-454 (2004), pp. 383–387. ISSN: 0040-6090. DOI: 10.1016/j.tsf.2003.11.161.

[24] Senthilkumar Alagesan et al. *Enhancement strategies for mesenchymal stem cells and related therapies*. Dec. 2022. DOI: 10.1186/s13287-022-02747-w.

[25] Gavin D.M. Jeffries et al. “3D micro-organisation printing of mammalian cells to generate biological tissues”. In: *Scientific Reports* 10.1 (Dec. 2020). ISSN: 20452322. DOI: 10.1038/s41598-020-74191-w.

[26] Pedro C. Chagastelles and Nance B. Nardi. *Biology of stem cells: An overview*. Sept. 2011. DOI: 10.1038/kisup.2011.15.

[27] Imran Ullah, Raghavendra Baregundi Subbarao, and Gyu Jin Rho. “Human mesenchymal stem cells - current trends and future prospective”. In: *Bioscience Reports* 35.2 (Apr. 2015), e00191. ISSN: 0144-8463. DOI: 10.1042/BSR20150025.

[28] L S Litvinova et al. “Human Mesenchymal Stem Cells as a Carrier for a Cell-Mediated Drug Delivery”. In: *Frontiers in Bioengineering and Biotechnology* 10 (2022). ISSN: 2296-4185. DOI: 10.3389/fbioe.2022.796111.

[29] Timothy E.G. Krueger et al. *Concise Review: Mesenchymal Stem Cell-Based Drug Delivery: The Good, the Bad, the Ugly, and the Promise*. Sept. 2018. DOI: 10.1002/sctm.18-0024.

[30] Abdullah Aldahmash et al. “Human Stromal (Mesenchymal) Stem Cells: Basic Biology and Current Clinical Use for Tissue Regeneration”. In: *Annals of Saudi Medicine* 32.1 (2012), pp. 68–77. DOI: 10.5144/0256-4947.2012.68.

[31] Shuyu Tian, Hong Zhao, and Nastassja Lewinski. “Key parameters and applications of extrusion-based bioprinting”. In: *Bioprinting* 23 (2021). ISSN: 2405-8866. DOI: 10.1016/j.bprint.2021.e00156.

[32] Shahrzad Rahmani et al. “Chapter 7 - Polymer nanocomposites for biomedical applications”. In: *Fundamentals of Bionanomaterials*. Ed. by Ahmed Barhoum, Jaison Jeevanandam, and Michael K Danquah. Micro and Nano Technologies. Elsevier, 2022, pp. 175–215. ISBN: 978-0-12-824147-9. DOI: 10.1016/B978-0-12-824147-9.00007-8.

[33] Naside Gozde Durmus et al. “Magnetic levitation of single cells”. In: *Proceedings of the National Academy of Sciences of the United States of America* 112.28 (July 2015), E3661–E3668. ISSN: 10916490. DOI: 10.1073/pnas.1509250112.

# A Details of the MTS/MTT plate arrangements

The focus of this appendix is to give further details of the plate arrangements used in the viability/survivability assays for hMSCs. The assay results of presented plates, in Table 2 below, are presented in Section 4 or in Appendix C.

**Table 2:** Four plate arrangements for viability/survivability assays for hMSCs

| Plate 1 - Viability control by MTS (Replicates: 4 wells, seeding: 10K cells/well) | Plate 2 - Viability control by MTT (Replicates: 4 wells, seeding: 10K cells/well ) | Plate 3 - Survivability control by MTS (Replicates: 6 wells, seeding: 10K cells/well) | Plate 4 - Viability control by MTS (Replicates: 6 wells) |
|---|---|---|---|
| Negative control | Negative control | Negative control | 1 000 cells in media |
| Histodenz 8 % [w/v] in media | Histodenz 8 % [w/v] in media | Histodenz 8 % [w/v] in media | 2 000 cells in media |
| Histodenz 18 % [w/v] in media | Histodenz 18 % [w/v] in media | Histodenz 18 % [w/v] in media | 5 000 cells in media |
| Histodenz 30 % [w/v] in media | Histodenz 30 % [w/v] in media | Histodenz 30 % [w/v] in media | 10 000 cells in media |
| Histodenz 40 % [w/v] in media | Histodenz 40 % [w/v] in media | Histodenz 40 % [w/v] in media | 20 000 cells in media |
| DMSO 0.1 % in media | DMSO 0.1 % in media | PBS (volume equal to Histodenz sample of 8 %) in media | Blank |
| DMSO 1 % in media | DMSO 1 % in media | PBS (volume equal to Histodenz sample of 18 %) in media | - |
| DMSO 10 % in media | DMSO 10 % in media | PBS (volume equal to Histodenz sample of 30 %) in media | - |
| Positive control | Positive control | PBS (volume equal to Histodenz sample of 40 %) in media | - |
| Blank | Blank | Positive control | - |
| - | - | Blank | - |

* Negative control: Media for hMSCs
* Positive control: 100 % DMSO
* Blank: Only sample withouth hMSCs, solely media for hMSCs

Table 2 presents vertically each plate set up for the viability tests (plate 1,2,4) and the survivability test (plate 3). The solutions listed for each plate (in 1-3) are the exposure mixtures, which was in contact with the cells for three hours. Plate 1 and 2 are duplicates analysed by MTS and MTT respectively. The DMSO was tested in different concentrations for methodology control, to check if the cells died gradually with the increased DMSO. In plate 3 the media dependence was assessed via exchange of Histodenz to PBS for all concentrations. Plate 1-3 was similar in terms of procedure with cell seeding and all had exposure mixtures. Plate 4 was a gradient plate with different seeding concentrations (hMSCs) and no exposure mixtures were used.

# B Size control of the recirculating fluid zone

This appendix presents the measurements of the recirculating fluid zone size, analysed, because of differences in printing solution viscosity when using PEG solution compared to Histodenz. In Figure 1 below, Histodenz concentration of 12 % [w/v] was tested against the control solution of PEG with a concentration of 1.5 % [w/v]. A fluorescent compound, added to each solution in equal volumes, allowed visualisation. The recirculating fluid zone measurements started when a 10 % increase in grey scale was obtained against the background (because of difficulties in determining where the fluorescence started) and ended at the printhead tip. The sizes of the recirculating fluid zones were found to be 76 $\mu$m for PEG and 67 $\mu$m of the Histodenz solution, which imply a slight difference in size. With a smaller recirculation zone, cells are printed over a smaller area which should be considered in the comparison of printability performance.

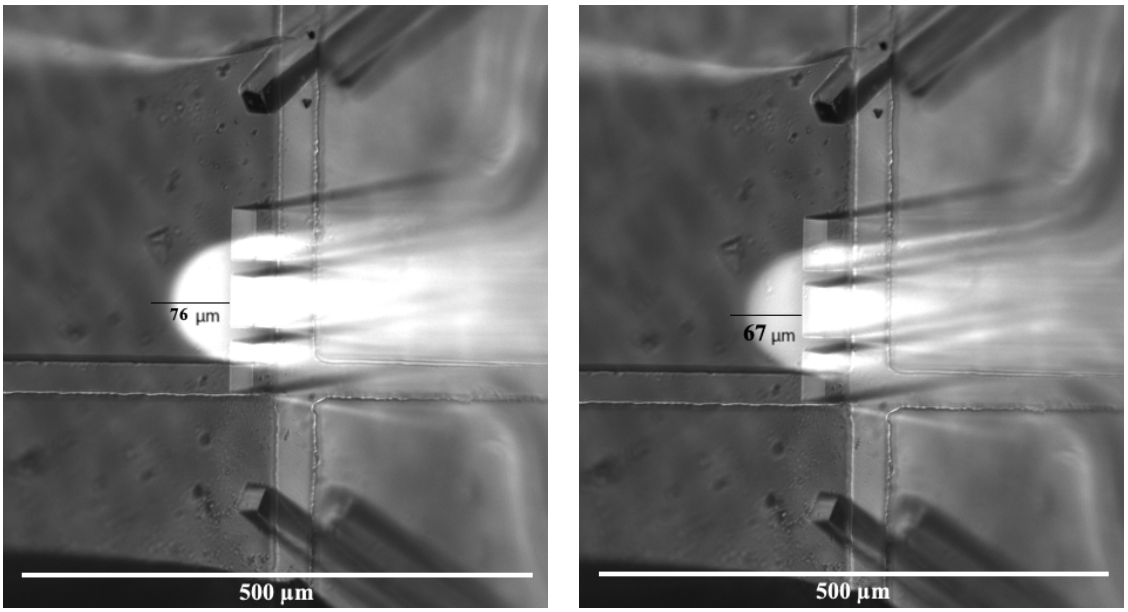


**(a)** PEG (1.5 % (w/v) in PBS) **(b)** Histodenz (12 % (w/v) in PBS)

**Figure 1:** Recirculating fluid zones at the printhead during printing of PEG and Histodenz, visualised with FITS. The control, PEG, was measured to a radius of 76 $\mu$m, while the Histodenz was measured to 67 $\mu$m.

# C Results of assay methodology control

The results presented in this appendix served as a methodology control for performed assays (MTS and MTT). In Figure 2 (a) the viability of hMSCs in DMSO is visualised. According to the data, the viability (%) decreases with increasing concentration of DMSO which assured the function of the positive control. In graph (b) the influence by different media volumes can be seen. Assessment of media dependence was required since the access to media for the cells were not equal for every solution exposure. By the values, the different volumes of media does not seem to impact the results (bars fairly stable). Lastly, Figure 2 (c) was performed to check the signal of the plate reader, to ensure its function. The signal was increasing with seeding density which was expected. In all, the methodology was evaluated to give reliable results.

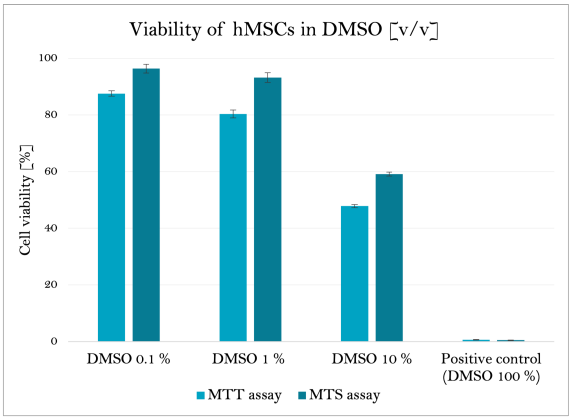


**(a)** Viability of hMSCs in DMSO (0.1 %, 1 %, 10 % and 100 %). Data obtained from both MTS and MTT assays. N=4 wells.

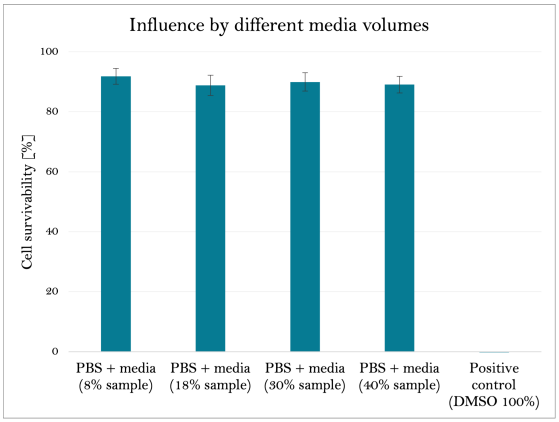


**(b)** Media dependence for the Histodenz samples, obtained via exchange of Histodenz volume to PBS in each sample. N=6 wells.

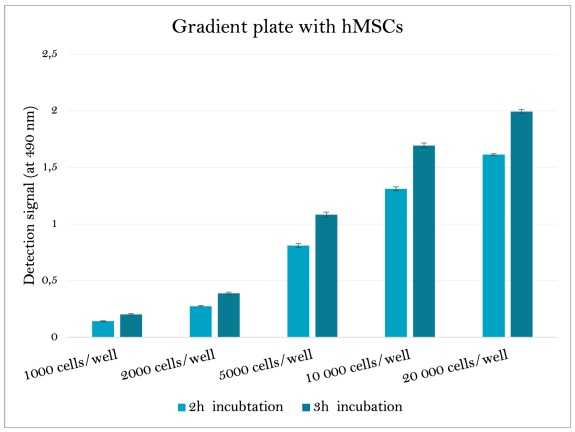


**(c)** Gradient seeded plate with hMSCs (1000, 2000, 5000, 10000 and 20000 cells/well respectively). N=6 wells.

**Figure 2:** The graphs presented in this figure serve as a methodology control for the viability/survivability assays. In (a-b) the bars are given as percentages of viable cells compared to the unexposed control group. In (c) the two bars for each seeding, give the detection signal (measured after two and three hours) obtained with the plate reader.

# D Emptied delivery chamber of printhead

In printability tests where printing stopped after an increased amount of cells were printed, all replicates had depletion of liquid in the delivery chamber, visualised in Figure 3. It occurred for all replicates of Histodenz solution 12 % and once for 8 %. As seen, the delivery chamber (1) is emptied. Important is also that the waste chambers for recirculation (7-8) are full.

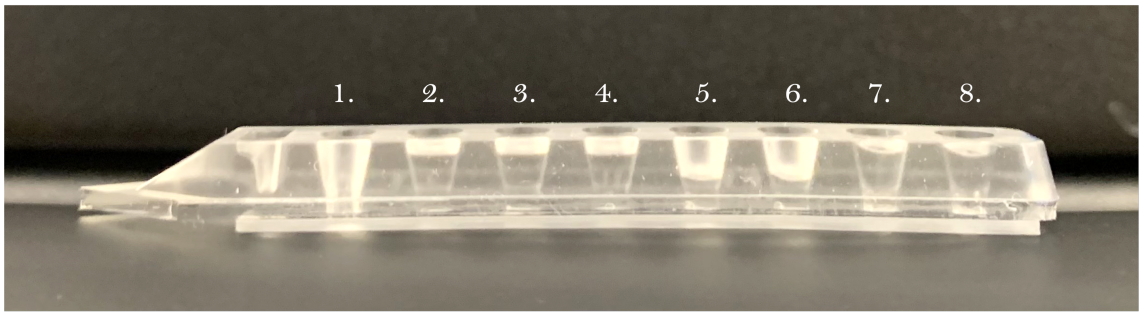


**Figure 3:** Picture of a printhead used in printing strategy 1, where the printing reached the increase in cell count before it stopped. Chamber 1 was used as the delivery chamber, containing hMSCs in Histodenz, and a meniscus cannot be recognised (empty). In the non-delivery chambers (2-3) the volume are remained high. The waste chambers for the switch (6-7) are not full compared to (7-8) the waste from the recirculation.

A recording captured the end of a printing test, using Histodenz solution 8 % [w/v], that started to print an increased amount of cell. In Figure 4, screenshots of the recording are presented. In (a) the printing gave increased cell density and aggregates of cells can be seen. In (b) the first air flows out of the printhead tip and in (c) the air bubbles are clearly shown after the manually stopped printing.

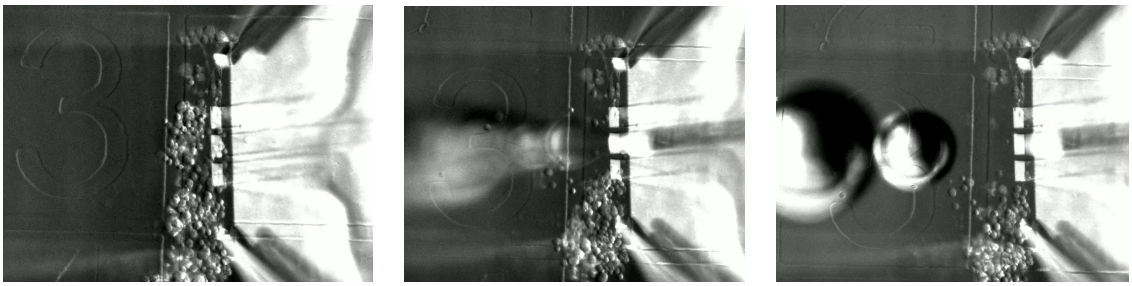

**(a)** Increased cell density printed

**(b)** Air flow out of the printhead tip

**(c)** Air bubbles after stopped printing

**Figure 4:** Screenshots from a recording of printing cells with Histodenz, where the printing gives increased cell density prior to depletion of volume in chamber.

**DEPARTMENT OF BIOLOGY AND BIOLOGICAL ENGINEERING**
**CHALMERS UNIVERSITY OF TECHNOLOGY**
Gothenburg, Sweden
www.chalmers.se


CHALMERS
UNIVERSITY OF TECHNOLOGY